

Springer Geology

Soumyajit Mukherjee

Atlas of Shear Zone Structures in Meso-scale

 Springer

Springer Geology

For further volumes:
<http://www.springer.com/series/10172>

Soumyajit Mukherjee

Atlas of Shear Zone Structures in Meso-scale

 Springer

Soumyajit Mukherjee
Department of Earth Sciences
Indian Institute of Technology Bombay
Mumbai, Maharashtra
India

ISBN 978-3-319-00088-6 ISBN 978-3-319-00089-3 (eBook)
DOI 10.1007/978-3-319-00089-3
Springer Cham Heidelberg New York Dordrecht London

Library of Congress Control Number: 2013951134

© Springer International Publishing Switzerland 2014

This work is subject to copyright. All rights are reserved by the Publisher, whether the whole or part of the material is concerned, specifically the rights of translation, reprinting, reuse of illustrations, recitation, broadcasting, reproduction on microfilms or in any other physical way, and transmission or information storage and retrieval, electronic adaptation, computer software, or by similar or dissimilar methodology now known or hereafter developed. Exempted from this legal reservation are brief excerpts in connection with reviews or scholarly analysis or material supplied specifically for the purpose of being entered and executed on a computer system, for exclusive use by the purchaser of the work. Duplication of this publication or parts thereof is permitted only under the provisions of the Copyright Law of the Publisher's location, in its current version, and permission for use must always be obtained from Springer. Permissions for use may be obtained through RightsLink at the Copyright Clearance Center. Violations are liable to prosecution under the respective Copyright Law. The use of general descriptive names, registered names, trademarks, service marks, etc. in this publication does not imply, even in the absence of a specific statement, that such names are exempt from the relevant protective laws and regulations and therefore free for general use.

While the advice and information in this book are believed to be true and accurate at the date of publication, neither the authors nor the editors nor the publisher can accept any legal responsibility for any errors or omissions that may be made. The publisher makes no warranty, express or implied, with respect to the material contained herein.

Printed on acid-free paper

Springer is part of Springer Science+Business Media (www.springer.com)

*I dedicate this book in memory of
my maternal grandfather late
Mr. Ranendra Kumar Banerjee*

Preface

Interpretation of structures from field is an integral part of structural geology. While research papers cannot display morphologic variations of individual structures, an atlas of field structural snaps remained due. This book fills up that gap. I have drawn most examples from western Himalayan shear zones. The reader is suggested to consult the key papers in the 'References' section for more information. I welcome comments and counterarguments at: soumyajitm@gmail.com

Acknowledgments

Thanks to all my students who sought alternate explanations on structures in the field. In particular, discussions Narayan Bose and Gourab Bhattacharya (IIT Bombay) were fruitful. Editorial handling by Sai Naren Ravisekhar, Varddhene V, Annett Buettner and Janet Steritt (Springer). Mentored by Chris Talbot (retired from Uppsala University). I am grateful to the staff members Bhim Bhatt (IIT Roorkee), Niranjana Panda (IIT Bombay), and Sher Singh Negi (Pooh village, Himachal Pradesh) for assisting several fieldworks in the Himalaya and elsewhere. Thanks to my wife Payel Mukherjee for her patience and support.

Contents

1 Ductile Shear	1
References	29
2 Folds	31
References	48
3 Veins and Near Symmetric Clasts	51
References	69
4 Boudins	71
References	85
5 Brittle Shear	87
References	124

Chapter 1

Ductile Shear

Ductile shear can host economically important minerals (Upton and Craw 2013). S–C fabrics (Bèrthe et al. 1979; Mukherjee 2011; Figs. 1.1, 1.2, 1.3, 1.4, 1.5, 1.6, 1.7, 1.8, 1.9, 1.10, 1.11, 1.12, 1.13, 1.14, 1.15, 1.16, 1.17, 1.18, 1.19, 1.20, 1.21, 1.22, 1.23, 1.24, 1.25, 1.26, 1.27, 1.28, 1.29, 1.30 and 1.31) and sheared clasts (Passchier and Trouw 2005; Figs. 1.32, 1.33, 1.34, 1.35, 1.36, 1.37, 1.38, 1.39, 1.40, 1.41, 1.42, 1.43, 1.44, 1.45, 1.46, 1.47, 1.48, 1.49, 1.50) are the commonest ductile shear sense indicators in meso-scale. Sigmoid-shaped or sigma structures of clasts are most common (Figs. 1.32, 1.33, 1.34, 1.35, 1.36, 1.37, 1.38, 1.39, 1.40, 1.41, 1.42, 1.43, 1.44, 1.45, 1.46, 1.47). On the other hand, delta structures are rather rare (Fig. 1.50). Secondary ductile shears (Figs. 1.5, 1.12, 1.14, 1.15, 1.17) indicate a pure shear component, besides simple shear, within the shear zone (Goscombe et al. 2006). Presence of granitic melt/leucosome at both S- and C-planes indicate possibly a syn-shearing migmatization (Marchildon and Brown 2003; Misra et al. 2009; especially Figs. 1.3, 1.4, 1.5, 1.9, 1.14, 1.15, 1.17, 1.20, 1.23, 1.25). Unlike tectonic simple shear (Mukherjee 2012), magma flows can locally induce ductile shear. The most ubiquitous manifestation of this are sheared vesicles (Philpotts and Ague 2005; Misra 2013; etc.; Figs. 1.51, 1.52, 1.53, 1.54). For reviews on S–C fabrics, see structural geological text books such as Davis et al. (2012). In terms of tectonics, ductile shear fabrics from the Greater Himalayan Crystallines indicate a top-to-S/SW fore-shear, which has also been well documented also under microscale (e.g. Mukherjee 2013a). Additionally, from the South Tibetan Detachment, a top-to-N/NE extensional shear is also reported, which has recently been explained by a combination of crustal channel flow and critical taper mechanisms (Beaumont and Jamieson 2010; recent review by Mukherjee and Ghosh 2013).



Fig. 1.1 *Top-to-left* ductile sheared sigmoidal S-fabrics bound by sub-horizontal shear C-planes. Near Kali Mitti Bridge, on National Highway 22A, Rampur district, Himachal Pradesh, Greater Himalayan Crystallines, India



Fig. 1.2 *Top-to-left (down)* ductile sheared quartzofeldspathic minerals define S-fabrics. These are bound by left dipping biotite foliations that define C-planes. Ambaji, Gujrat, India



Fig. 1.3 *Top-to-right* ductile sheared S-fabric bound by leftward converging non-parallel C-planes. *At right* a thick sigmoid leucosome body defines a prominent S-fabric. Migmatite from the Greater Himalayan Crystallines, India. Reproduced from Fig. 3a of Mukherjee (2010)



Fig. 1.4 A zone of close-spaced thinner melanosomes and few thicker leucosomes occur as a lens in the *bottom* and the *central part* of the photo and define S-planes. *Top-to-right (up)* ductile sheared. These S-planes are curved only near the C-planes. This lens is bound by thicker leucosome layers. Above this, curved close-spaced C-planes bound S-fabrics of nearly sigmoidal quartz pods. Greater Himalayan Crystallines, Sulej section, India. Reproduced from Fig. 4c of Mukherjee (2010)



Fig. 1.5 *Top-to-right* ductile sheared thicker leucosomes and thinner melanosomes. *Top-to-right (down)* synthetic secondary C' shear also developed. Reproduced from Fig. 4a of Mukherjee and Koyi (2010)



Fig. 1.6 *Top-to-right* sheared migmatite with thicker leucosomes and thinner melanosomes. The C -plane of ductile shear is nearly horizontal and is *marked by the pen*. Leucosomes that define the S -planes are of varying thickness. Greater Himalayan Crystallines, Sutlej section, Himachal Pradesh, India



Fig. 1.7 S-fabrics and intrafolial folds of leucosomes consistently indicate a *top-to-right (up)* ductile shear. Both the C- and the S-planes dip towards *left*. However, the S-planes are steeper. Secondary synthetic shear planes (C') exist. Ductile sheared migmatite from Greater Himalayan Crystallines, Sutlej section, Himachal Pradesh, India



Fig. 1.8 *Top-to-left (up)* ductile sheared migmatite with thicker leucosome and thinner melanosome layers. The C-planes are sub-horizontal. Greater Himalayan Crystallines, Sutlej section, Himachal Pradesh, India

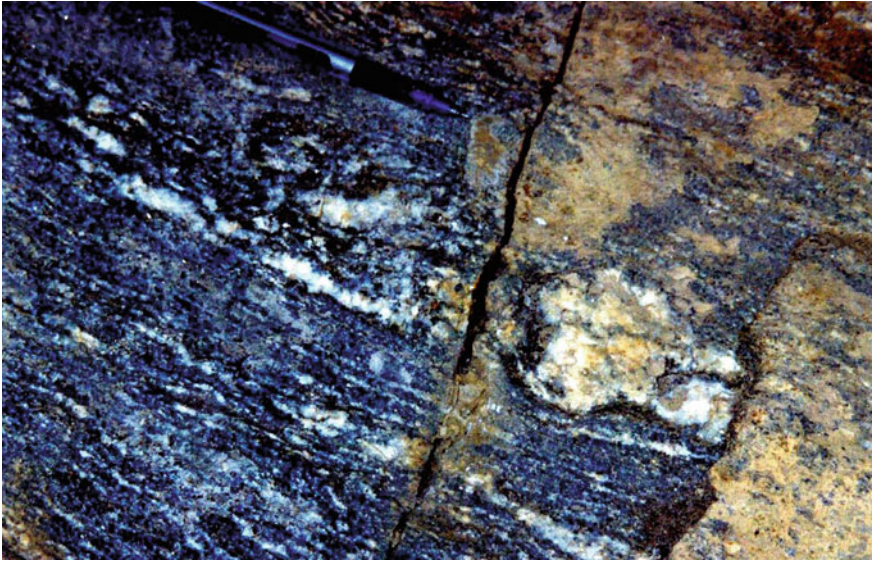


Fig. 1.9 *Top-to-right (down)* ductile sheared S-fabrics defined by leucosomes. Nearly straight C-planes dip towards *right*. Located between Pangi and Kashang bridges, Sutlej section of Greater Himalayan Crystallines. Reproduced from Fig. 5a of Mukherjee and Koyi (2010)



Fig. 1.10 *Top-to-right (down)* ductile sheared S-fabrics defined by leucosomes. Nearly straight C-planes dip towards *right*. Sutlej section of Greater Himalayan Crystallines, Himachal Pradesh, India. Reproduced from Fig. 5b of Mukherjee and Koyi (2010)

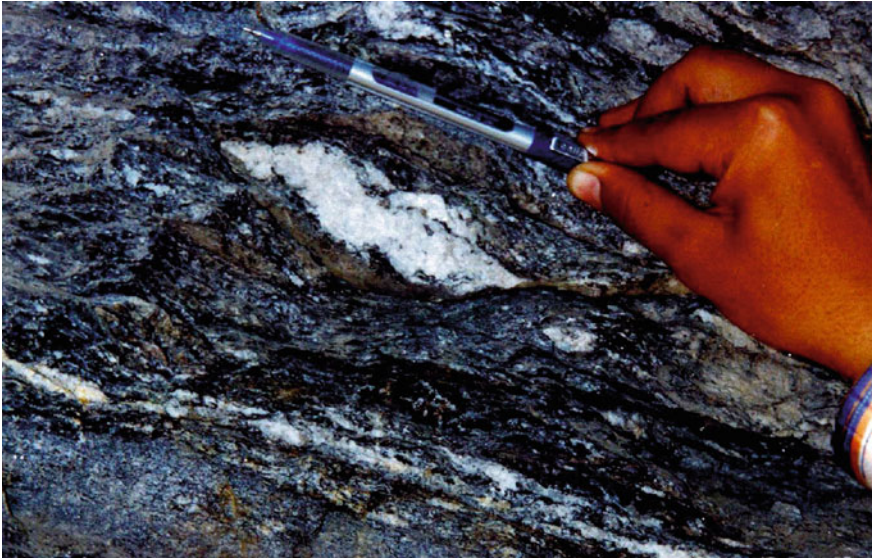


Fig. 1.11 *Top-to-left* ductile sheared leucosome pod define the S-fabric. Sub-horizontal C-plane. Sutlej section of Greater Himalayan Crystallines, Himachal Pradesh, India

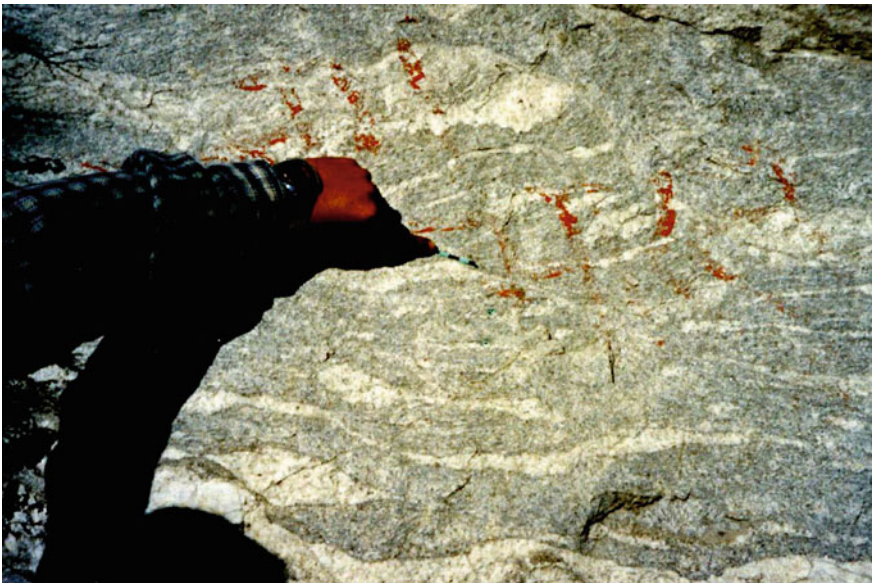


Fig. 1.12 *Top-to-right* and *top-to-right (down)* ductile sheared leucosome layers. Near Kharo bridge, Sutlej section of Greater Himalayan Crystallines, Himachal Pradesh, India. Reproduced from Fig. 5d of Mukherjee and Koyi (2010)



Fig. 1.13 *Top-to-left (up)* ductile sheared S-planes defined by thicker leucosomes and thinner melanosomes. Thin sharp straight C-plane dips towards *right*. Between Kashang and Kharo bridges, Sutlej section of Greater Himalayan Crystallines, Himachal Pradesh, India. Reproduced from Figs. 4d and 5c, d of Mukherjee and Koyi (2010)

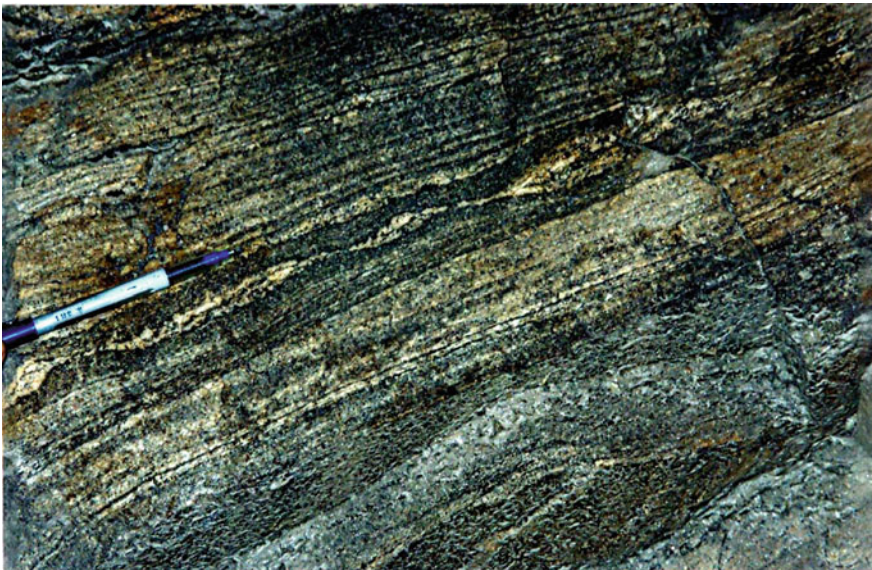


Fig. 1.14 A train of *top-to-right (up)* sheared quartz rich sigmoid ductile sheared pods. Primary C-shear acted along the left dipping foliation planes. Synthetic secondary C' acted along the short straight tails through which individual sigmoids are interconnected. From mylonitized gneiss/migmatite of Greater Himalayan Crystallines, Sutlej section, India

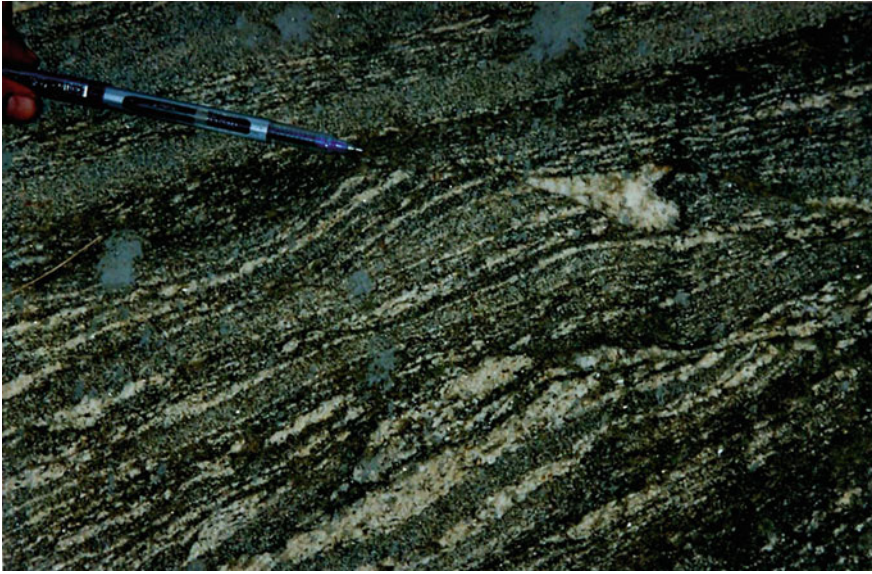


Fig. 1.15 *Top-to-right (down)* ductile sheared S-fabrics are defined by a part of foliations of quartzo-feldspathic minerals and biotites. *Note* accumulation of quartz of irregular geometry along C-plane. Mylonitized gneiss/migmatite of Greater Himalayan Crystallines, Sutlej section, India



Fig. 1.16 Rootless sigmoidal quartz veins and overturned folded veins indicate consistently a *top-to-right* shear. Greater Himalayan Crystallines, Sutlej section, India



Fig. 1.17 A ductile shear oblique to the left dipping main foliation along sharp short straight lines affected quartz rich foliations giving rise to diverse shapes. From mylonitized gneiss/migmatite of Greater Himalayan Crystallines, Sutlej section, India



Fig. 1.18 *Top-to-right* sheared sigmoid quartz veins in several zones. Greater Himalayan Crystallines, Sutlej section, India



Fig. 1.19 Asymmetric quartz pods indicate both primary *top-to-right-down* (C, blue half arrow) and synthetic secondary (C', green half arrow) ductile shear. Here the C-planes dip towards *right*. From mylonitized gneiss/migmatite of Greater Himalayan Crystallines, Sutlej section, India



Fig. 1.20 A number of sigmoid quartz pods that act as ductile shear S-fabric reveal a *top-to-right (down)* shear. Exact geometries and in some cases sizes of individual sigmoids vary. An overturned round hinge intrafolial fold also shows the same shear sense. From mylonitized gneiss/migmatite of Greater Himalayan Crystallines, Sutlej section, India. Reproduced from Fig. 1.5d of Mukherjee (2010)



Fig. 1.21 *Top-to-left* ductile shear indicated by sigmoid-shaped leucosomes. Thin melanosomes within leucosomes also define S-fabrics. The ductile shear C-planes are sub-horizontal and wavy. Near Pangri, Sutlej section of Greater Himalayan Crystallines, Himachal Pradesh, India. Reproduced from Fig. 1.4d of Mukherjee and Koyi (2010)



Fig. 1.22 Weavy sub-horizontal C-planes. *Top-to-left* shear given by sigmoid quartz veins near the *center* and the *top* parts of the photo. Greater Himalayan Crystallines, Sutlej section, India

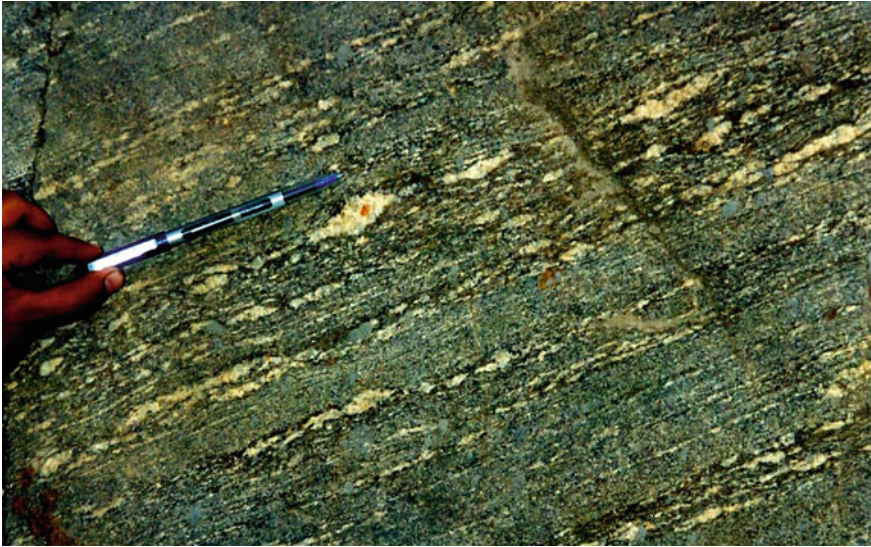


Fig. 1.23 *Top-to-right (up)* ductile sheared sigmoid quartz veins in several zones. A few quartz veins parallel the C-planes. Greater Himalayan Crystallines, Sutlej section, India



Fig. 1.24 A train of interconnected sigmoid shaped quartz pods define a *top-to-left (up)* ductile shear. Bottom left to this, foliation boudins developed. No fabrics visible inside these sigmoids and boudins. From mylonitized gneiss/migmatite of Greater Himalayan Crystallines, Sutlej section, India. Isolated sub-rounded and sigmoidal quartz veins define the shear fabrics



Fig. 1.25 *Top-to-right (down)* sheared quartz veins in a mylonitized gneiss. Bhagirathi section of Greater Himalayan Crystallines, India. Reproduced from Fig. 3b of Mukherjee (2013b)



Fig. 1.26 *Top-to-left (up)* ductile sheared foliations. A few quartzofeldspathic layers are like sigma-structures. Bhagirathi section of Greater Himalayan Crystallines, India

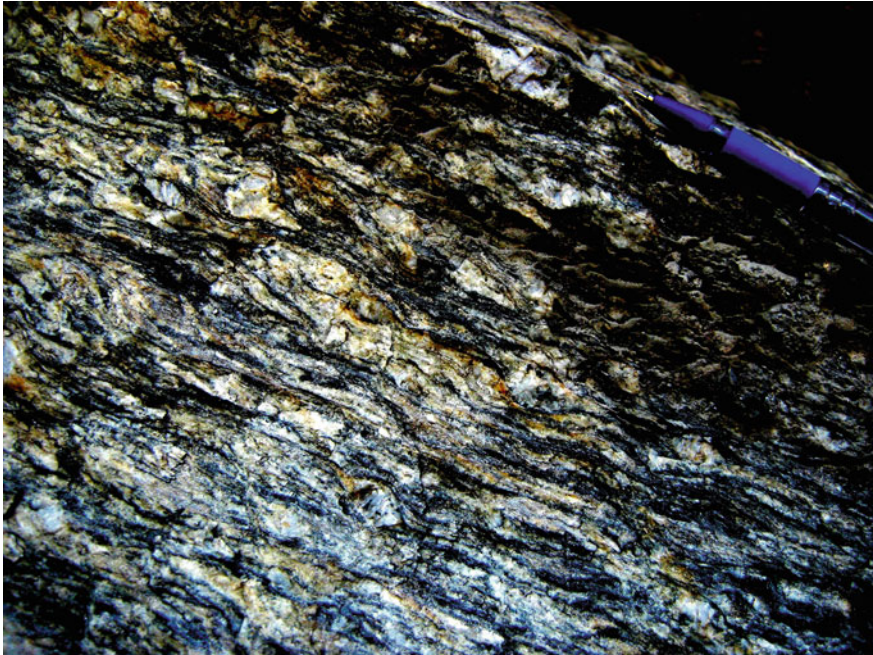


Fig. 1.27 Weavy foliations in a mylonitized gneiss. No clear cut shear sense revealed. Greater Himalayan Crystallines, Sutlej section, India



Fig. 1.28 *Top-to-left (down)* sheared quartz and feldspar clasts bound by straight C-planes of ductile shear. Some of the sheared fabrics within the C-planes are folded. Greater Himalayan Crystallines, Sutlej section, India



Fig. 1.29 *Top-to-right (down)* ductile sheared C-planes restricted near right dipping C-planes. Tethyan Sedimentary Zone. Sutlej section, India

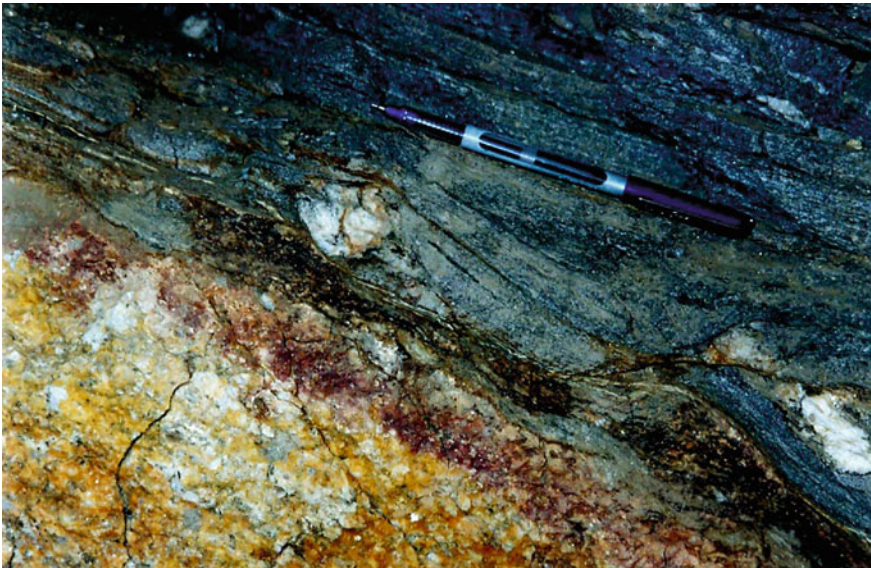


Fig. 1.30 *Top-to-left* (brittle/ductile?) sheared foliations from mylonitized gneiss/migmatite of Greater Himalayan Crystallines, Sutlej section, India. Isolated sub-rounded and sigmoidal quartz veins define the shear fabrics. Reproduced from Fig. 23b of Mukherjee (2010)



Fig. 1.31 Black (burnt?) lithology within migmatitic gneiss shows a *top-to-left (up)* shear. Within individual bulges of *yellowish rock* that define S-fabrics, complicated internal fabrics also seen. Greater Himalayan Crystallines, Sutlej section, Himachal Pradesh, India



Fig. 1.32 An aggregate of quartz grains with irregular margins define a sigmoid shape and indicate a *top-to-right* ductile shear. It resembles microscopic composite sigmoid fish of Mukherjee (2011). From mylonitized gneiss/migmatite of Greater Himalayan Crystallines, Sutlej section, Himachal Pradesh, India



Fig. 1.33 A *top-to-right* ductile sheared leucosome pod defines the S-fabric. Its tail at left parallels and defines the C-plane. Greater Himalayan Crystallines, Sutlej section, Himachal Pradesh, India



Fig. 1.34 A *top-to-left* ductile sheared sigmoid quartz pod defines the S-fabric. Its left tip is of uncommon morphology. From mylonitized gneiss/migmatite of Greater Himalayan Crystallines, Sutlej section, Himachal Pradesh, India. Reproduced from Fig. 2c of Mukherjee (2010)



Fig. 1.35 An S-fabric defined by quartz vein and biotites. Pulled margins of the vein along the C-planes at opposite corners helps identify the C-planes easily. *Top-to-left (up)* shear sense. Greater Himalayan Crystallines, Sutlej section, Himachal Pradesh, India



Fig. 1.36 A sigmoid/parallelogram rootless quartz vein. *Top-to-right (down)* shear. Much thinner isolated white quartz veins at left define the same shear sense. Near Karcham hydropower plant. Greater Himalayan Crystallines, Sutlej section, Himachal Pradesh, India



Fig. 1.37 *Top-to-left (up)* ductile sheared sigmoid-shaped quartz veins (with notches at corners). The C-planes of ductile shear dips towards right. Greater Himalayan Crystallines, Sutlej section, Himachal Pradesh, India. Reproduced from Fig. 6c of Mukherjee and Koyi (2010)



Fig. 1.38 *Top-to-right (up)* sheared sigmoid pods of quartz veins define the sheared S-planes within mylonitized gneiss. The C-planes dip towards left. *Right to the pen*, mylonitic/gneissic foliation are brittle normal faulted. Greater Himalayan Crystallines, Sutlej section, Himachal Pradesh, India. Reproduced from Fig. 6d of Mukherjee and Koyi (2010)



Fig. 1.39 *Top-to-right (down)* ductile sheared quartz veins defines the S-planes of various aspect ratios. The C-planes dip towards *right*. Greater Himalayan Crystallines, Sutlej section, Himachal Pradesh, India. Reproduced from Fig. 6b of Mukherjee and Koyi (2010)



Fig. 1.40 A *top-to-left* ductile sheared clast resembles a sigma structure. Its parallel tails define the ductile shear C-planes. Mylonitized gneiss from Greater Himalayan Crystallines, Bhagirathi section, India



Fig. 1.41 *Top-to-right (up)* ductile sheared quartz pod within mylonitized gneiss. The mylonitic foliations defined by thinner biotite and thicker quartzofeldspathic minerals dip towards right. Greater Himalayan Crystallines, Bhagirathi section, India



Fig. 1.42 A symmetric clast within mylonitized gneiss does not give any ductile shear sense. However, a few adjacent clasts reveal a *top-to-left (up)* ductile shear along right dipping foliation planes (= C-planes). Greater Himalayan Crystallines, Bhagirathi section, India



Fig. 1.43 *Top-to-left (up)* ductile sheared clast of quartz. Alternate layers of biotites and quartzofeldspathic minerals define mylonitic foliation. Note the tail in bottom is much longer than that at top. Sheared gneiss from Bhagirathi section of Greater Himalayan Crystallines, India



Fig. 1.44 A sheared feldspar clast. Shear sense is ambiguous. Biotites and elongated quartz define the C-planes that dip towards right. Greater Himalayan Crystallines, Bhagirathi section, India



Fig. 1.45 A rootless sigmoid quartz vein defines S-plane of ductile shear. Schistosity defines the *top-to-left* (*up*) primary shear C-plane. Bhagirathi section of Greater Himalayan Crystallines, India



Fig. 1.46 A *top-to-right* (*down*) ductile sheared quartz pod with strong asymmetry restricted at its tails. The main body of the clast is sub-rounded. A thick layer of biotite defines the C-plane more prominently left to the clast. Reproduced from Fig. 4c of Mukherjee (2013b). Bhagirathi section of Greater Himalayan Crystallines, India



Fig. 1.47 A sigma structure of quartz vein. *Top-to-left (up)* ductile sheared. Close spaced quartzofeldspathic minerals and biotites define the mylonitic foliations. A fracture at $\sim 90^\circ$ cut across the mylonitic foliations and the clast. Bhagirathi section of Greater Himalayan Crystallines, India

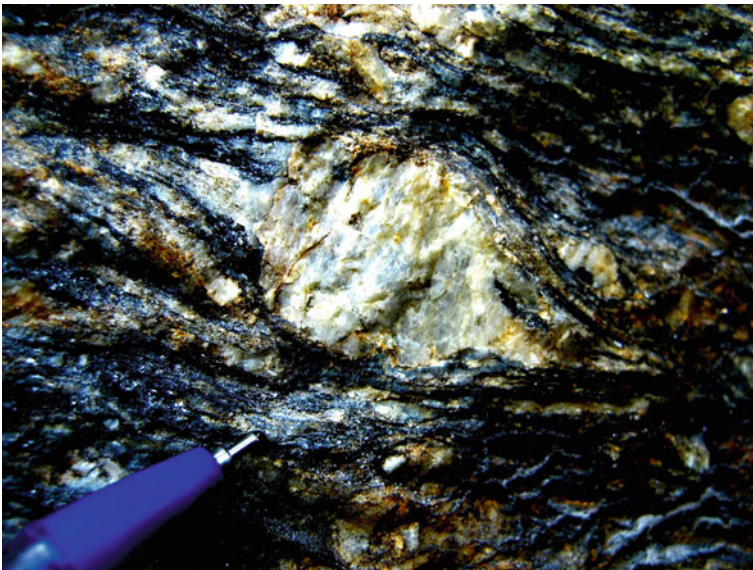


Fig. 1.48 A sigma structure of feldspar clast. *Top-to-left* sheared. Primary shear C-planes nearly horizontal. *Note* the two tails are of different geometries. Greater Himalayan Crystallines, Bhagirathi section, India

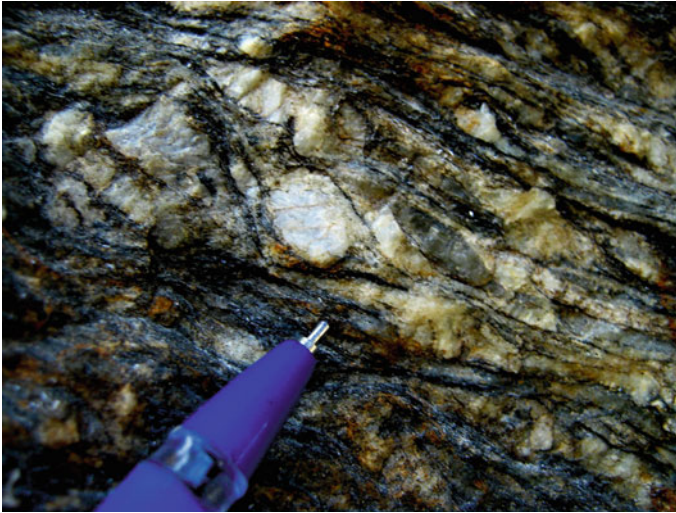


Fig. 1.49 A delta structure of quartz clast. *Top-to-left (up)* ductile sheared. Reproduced from Fig. 2b of Mukherjee (2013b). From mylonitized gneiss at Bhagirathi section of Greater Himalayan Crystallines, India



Fig. 1.50 A *top-to-left (down)* ductile sheared delta structure of quartz vein. Its tails merge with the primary shear C-planes (= gneissosity = mylonitic foliation = main foliation) of the mylonitized gneiss. Delta structures are observed rarely from meso- and micro-scales, and indicate usually a high strain (Passchier and Trouw 2005). A vein developing a delta structure probably has not been reported previously, except 1.4d of Mukherjee (2013b) from where this figure is reproduced. Notice that (1) at *top left* of the delta structure, an asymmetric quartz pod demonstrate the same shear sense; (2) when the tails and the clast are of the same minerals and both define a delta geometry, it has been described as a '*rolling structure*' (Driessche and Brun 1996). Bhagirathi section of Greater Himalayan Crystallines, India



Fig. 1.51 A basalt flow layer consisting of curved sheared elongated zeolite vesicles. Comparing these sheared vesicles with S-fabric's curvature, we can assign a top-to-left shear. However, this deformation is most likely to be due to lava flow and is not related to tectonics. Deccan trap basalt at Malsejghat, Maharashtra



Fig. 1.52 'Arrow-head' zeolite vesicles from the Deccan trap basalt at Malsejghat, Maharashtra. Curved internally strained individual zeolite vesicles define limbs of individual arrows. Does this indicate a flow of lavas from right to left? Deccan trap basalt at Malsejghat, Maharashtra



Fig. 1.53 Sheared, curved, internally strained zeolite vesicles possibly indicate a *top-to-left* local shear due to lava flow. A few vesicles resemble folds. However, those could be due to coalescence of gas bubbles when they tried to escape upwards from hot lava. Note a few nearly straight vesicles at the left portion of the photo. Deccan trap basalt at Malsejghat, Maharashtra



Fig. 1.54 'Arrow-head' zeolite vesicles as described previously in 1.52. 'Folded vesicle' as described in 1.53. Deccan trap basalt at Malsejghat. Maharashtra

References

- Beaumont C, Jamieson RA (2010) Himalayan–Tibetan Orogeny: channel flow versus (critical) wedge models, a false dichotomy? In: Leech ML et al (eds) Proceedings for the 25th Himalaya-Karakoram-Tibet workshop: U.S. Geological Survey, Open-File Report
- Bèrthe D, Choukroune P, Jegouzo P (1979) Orthogneiss, mylonite and non-coaxial deformation of granite: the example of the south Armorican shear zone. *J Struct Geol* 1:31–42
- Davis GH, Reynolds SJ, Kluth CF (2012) Structural geology of rocks and regions. Wiley, New York
- Diessche JVD, Brun J-P (1996) Rolling structures at large shear strain. *J Struct Geol* 9:691–704
- Goscombe B, Gray D, Hand M (2006) Crustal architecture of the Himalayan metamorphic front in eastern Himalaya. *Gond Res* 10:232–255
- Marchildon N, Brown M (2003) Spatial distribution of melt-bearing structures in anatectic rocks from Southern Brittany, France: implications for melt transfer at grain- to orogen-scale. *Tectonophysics* 364:215–235
- Misra AA (2013) Photograph of the month. *J Struct Geol* (in press)
- Misra S, Burlini L, Burg J-P (2009) Strain localization and melt segregation in deforming metapelites. *Phys Earth Planet Inter* 177:173–179
- Mukherjee S (2010) Structures in Meso- and Micro-scales in the Sutlej section of the Higher Himalayan Shear Zone, Indian Himalaya. *e-Terra* 7:1–27
- Mukherjee S (2011) Mineral fish: their morphological classification, usefulness as shear sense indicators and genesis. *Int J Earth Sci* 100:1303–1314
- Mukherjee S (2012) Simple shear is not so simple! Kinematics and shear senses in Newtonian viscous simple shear zones. *Geol Mag* 149:819–826
- Mukherjee S (2013a) Deformation microstructures in rocks. Springer, Berlin, pp 1–111
- Mukherjee S (2013b) Higher Himalaya in the Bhagirathi section (NW Himalaya, India): its structures, backthrusts and extrusion mechanism by both channel flow and critical taper mechanisms. *Int J Earth Sci* 102:1851–1870
- Mukherjee S, Koyi HA (2010) Higher Himalayan shear zone, Sutlej section: structural geology and extrusion mechanism by various combinations of simple shear, pure shear and channel flow in shifting modes. *Int J Earth Sci* 99:1267–1303
- Mukherjee S, Ghosh R (2013) Both channel flow and critical taper operated on the Greater Himalayan Crystallines (GHC)—a review. In: 28th Himalaya Karakoram Tibet Workshop & 6th International Symposium on Tibetan Plateau 2013. Tuebingen University, Germany
- Passchier CW, Trouw RAJ (2005) *Microtectonics*, 2nd edn. Springer, Berlin
- Philpotts A, Ague J (2005) *Principles of igneous and metamorphic Petrology*. Cambridge University Press, Cambridge
- Upton P, Craw D (2013) Extension and gold mineralization in the hanging walls of active convergent continental shear zones. *J Struct Geol* (in press)

Chapter 2

Folds

Ductile shear related folds have been studied by many (e.g. Bell 2010 but many others). Alsop and Holdsworth (2004) classified folds in relation to shear of two main types: (1) those with low inter-limb angles and curved hinge lines formed before shear; and (2) flow perturbed syn-shear overturned intrafolial folds. Vergences of intrafolial folds reveal shear sense in meso- (Figs. 2.1, 2.2, 2.3, 2.4, 2.5, 2.6, 2.7, 2.8, 2.9, 2.10, 2.11, 2.12, 2.13, 2.14, 2.15, 2.16, 2.17, 2.18, 2.19, 2.20, 2.21, 2.22, 2.23, and 2.28; Mukherjee et al. 2013) and micro-scales (Mukherjee 2013a). Intrafolial folds with axial traces sub-parallel to the shear planes (Fig. 2.24) are not useful in shear sense determination. Folds that are not bound by a pair of ductile shear planes (Figs. 2.25, 2.26, 2.27, 2.28, 2.29, 2.30, 2.31, 2.32 and 2.33) are not intrafolial, and do not indicate any ductile shear. In terms of tectonics, intrafolial folds from the Greater Himalayan Crystallines indicate a top-to-S/SW fore-shear (see Mukherjee and Koyi 2010a, b; Mukherjee 2013a, b etc.). Additionally, from the South Tibetan Detachment, a top-to-N/NE extensional shear is also reported, which has recently been explained by a combination of crustal channel flow and critical taper mechanisms (Beaumont and Jamieson 2010; recent review by Mukherjee and Ghosh 2013).



Fig. 2.1 A train of intrafolial folds of quartz (*left*) merges to a sigmoidal bulge (*right*). Dip of axial planes of the folds and the asymmetry of the sigmoid indicate consistently a *top-to-right (up)* shear sense. *Location* Greater Himalayan Crystallines from Sutlej section, Himachal Pradesh, India



Fig. 2.2 An overturned intrafolial fold of quartzose layer. *Top-to-left (up)* ductile sheared. At Jeori, Sutlej section of Greater Himalayan Crystallines, Himachal Pradesh, India. Reproduced from Fig. 4c of Mukherjee and Koyi (2010a, b)



Fig. 2.3 Irregular inconsistent folds inside a mylonitized gneiss. The two fold closures near the *central part* of the photo have left dipping axial traces. *Location* Greater Himalayan Crystallines from Sutlej section, Himachal Pradesh, India

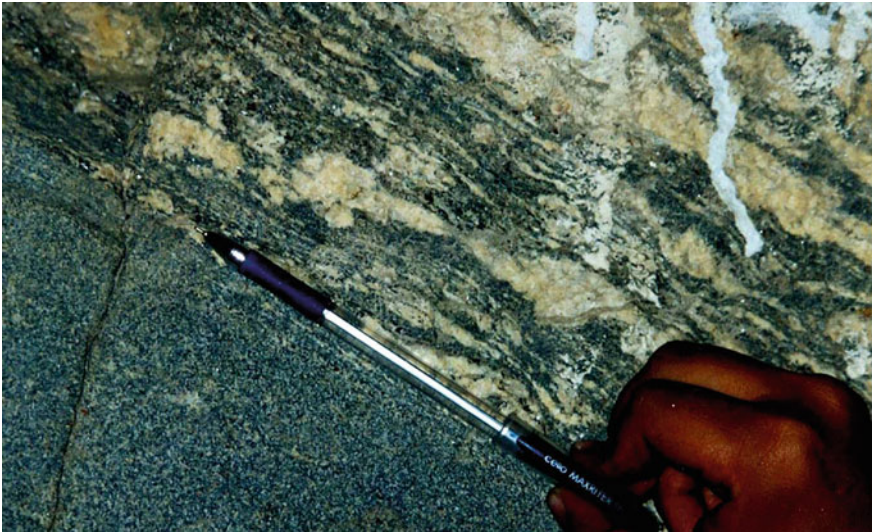


Fig. 2.4 Intrafolial folds of quartz veins with hinges thicker than the limbs. Since their axial traces sub-parallel the bounding nearly straight quartz veins defining primary shear C-planes, these folds cannot indicate any clear cut shear sense. Greater Himalayan Crystallines from Sutlej section, Himachal Pradesh, India



Fig. 2.5 *Hook-shaped round hinged folds of quartz veins. Axial traces of these folds sub-parallel the mylonitic foliations. Shear sense is not convincing. Ductile sheared migmatitic gneiss near an unnamed iron bridge at Karcham, Greater Himalayan Crystallines, Sutlej section, Himachal Pradesh, India*



Fig. 2.6 *Round-hinged overturned intrafolial folds of quartz veins indicate a top-to-left (down) ductile shear. Near Karcham hydropower plant, Sutlej section of Greater Himalayan Crystallines, Himachal Pradesh, India*



Fig. 2.7 Same description and location as the previous caption. A few folds have nearly *straight* hinge zones produced by ductile shear



Fig. 2.8 An overturned intrafolial fold of quartz vein follows nearly the same geometry of folding of gneissic foliation. *Top-to-right (up)* shear. At *right*, the folded vein merges with an irregular bulge of quartz. *Location* Karchham, near an unnamed iron bridge, Greater Himalayan Crystallines, Sutlej section, Himachal Pradesh, India

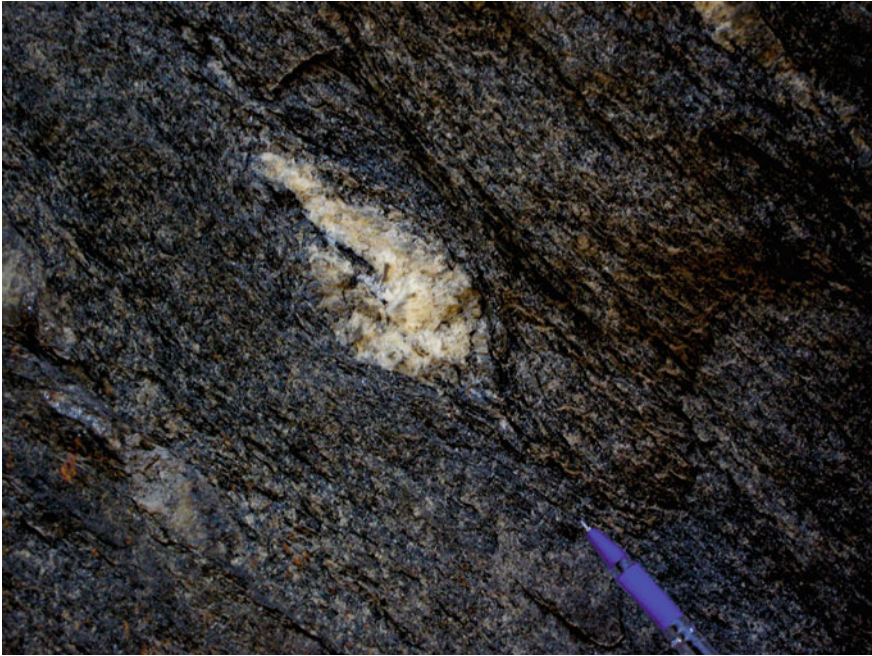


Fig. 2.9 A rootless fold of quartz with a hinge zone much thicker than the limbs. The axial trace sub-parallel the main foliation, and is therefore not a shear sense indicator. *Location* Greater Himalayan Crystallines, Bhagirathi section in India



Fig. 2.10 Overturned intrafolial folds of quartz veins with round hinges much thicker than the limbs. No clear-cut shear sense is revealed since the axial traces are at very low angles to the primary shear planes. From mylonitized gneiss/migmatite of Greater Himalayan Crystallines, Sutlej section, Himachal Pradesh, India. Reproduced from Fig. 17b of Mukherjee (2010). See Figs. 14.29 and 14.30 of Klein and Philpotts (2013) for similar cases



Fig. 2.11 *Top-to-right* sheared overturned intrafolial fold of quartz with round hinge. *Left* to it is an asymmetric quartz pod with mouth/notch at *right*. From mylonitized gneiss/migmatite of Greater Himalayan Crystallines, Sutlej section, Himachal Pradesh, India



Fig. 2.12 *Top-to-left (down)* ductile sheared thicker intrafolially folded leucosome layers. The *central part* of this photograph was published as Fig. 2.16d in Mukherjee (2010). Near Karcham, Greater Himalayan Crystallines, Sutlej section, Himachal Pradesh, India



Fig. 2.13 *Top-to-right (up)* ductile sheared migmatitic foliations. At places brittle rupture in the same shear sense took place. Greater Himalayan Crystallines, Sutlej section, Himachal Pradesh, India. Reproduced from Fig. 15d in Mukherjee (2010)



Fig. 2.14 Overturned intrafolial fold of quartz vein. *Top-to-right (up)* sheared. Pronounced shear led to boudinage. From mylonitized gneiss/migmatite of Greater Himalayan Crystallines, Sutlej section, India



Fig. 2.15 Isoclinally folded round hinged quartz vein. A few are *hook-shaped*. Notice at *bottom*, the fold cuts across the *left* dipping foliation. Hence these are not intrafolial folds, and are not to be considered as ductile shear sense indicators. From mylonitized gneiss/migmatite of Greater Himalayan Crystallines, Sutlej section, India

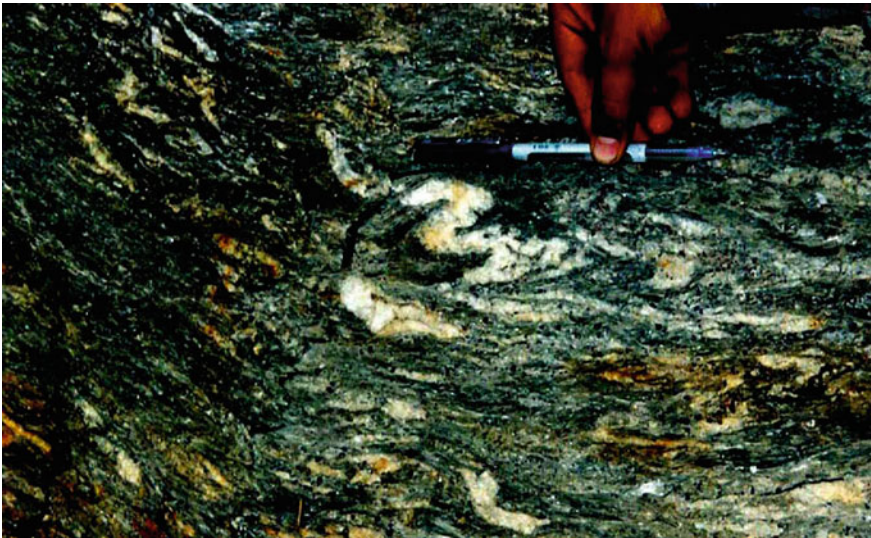


Fig. 2.16 Quartz vein folded with a vergence towards right. Shear sense is ambiguous since these folds are not bound by (nearly) *straight* shear C-planes. *Location* Greater Himalayan Crystallines from Sutlej section, Himachal Pradesh, India



Fig. 2.17 A tight polyclinally folded quartz vein cuts across foliations of mylonitized gneiss/migmatite. Since this fold is not bound by foliations, it is not to be considered an ‘intrafolial fold’, and therefore is not to be used as a shear sense indicator. Greater Himalayan Crystallines, Sutlej section, India. Reproduced from Fig. 15c of Mukherjee (2010)

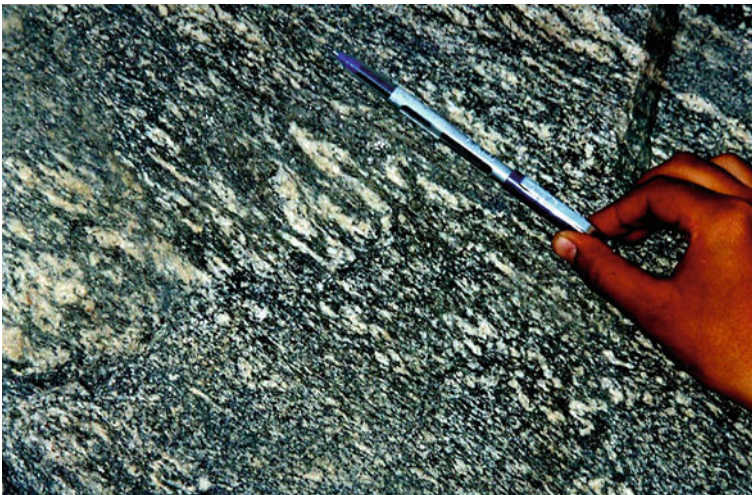


Fig. 2.18 Quartz-rich foliations at places show hook-fabric [see Wennberg (1996) for modeled—and Mukherjee and Koyi (2010b) for micro-scale examples]. Hook-fabrics are produced from pro- and retro- shear along the same primary shear C-planes. One can also work out the relative timing of the two shear sense from them. However, in the present case, the hook fabrics is seen to cut across the C-planes (= main foliations dipping towards right). So its origin might be different. From mylonitized gneiss/migmatite of Greater Himalayan Crystallines, Sutlej section, India. Reproduced from Fig. 14c of Mukherjee (2010)



Fig. 2.19 An isoclinally folded quartz vein resembling a ‘hook’ with hinge much thicker than the limbs. Since its axial trace parallels the main foliation, it cannot be used for ductile shear sense determination. Such parallel nature may be achieved if the fold underwent a protracted ductile shear. From mylonitized gneiss/migmatite of Greater Himalayan Crystallines, Sutlej section, India



Fig. 2.20 Folded quartz vein cuts across gneissic foliation, and is not bound by the later. Therefore these folds are not intrafolial and are to be avoided to determine shear sense. *Location* Karchham, near an unnamed iron bridge, Greater Himalayan Crystallines, Sutlej section, India

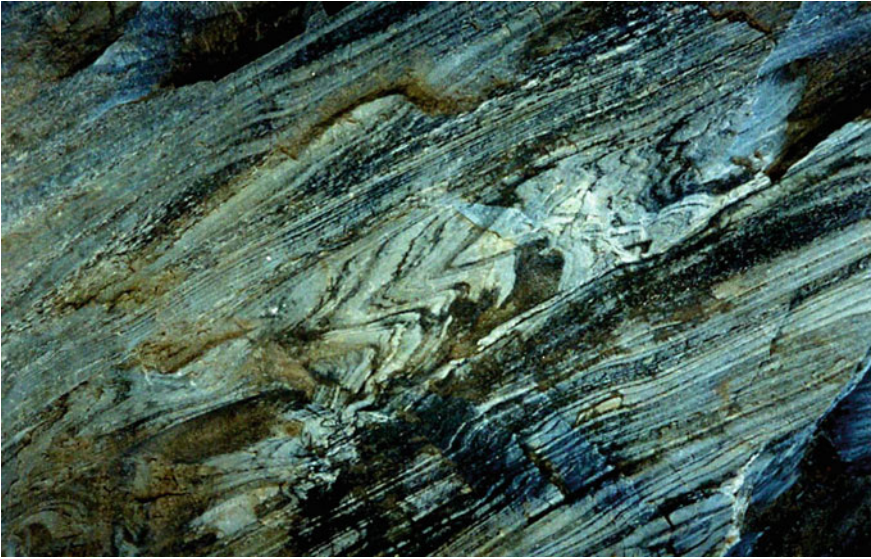


Fig. 2.21 A zone of folded gneissic foliation bound by nearly *straight sub-parallel* foliations. Axial traces of these folds sub-parallel those bounding foliations. Parasitic folds are also present. For these complications, these folds are to be avoided in shear sense determination. *Location* Karchham, near an unnamed iron bridge, Greater Himalayan Crystallines, Sutlej section, India



Fig. 2.22 *Left* verging folded quartz veins with hinge zones much thicker than the limbs. *Location* Greater Himalayan Crystallines, Bhagirathi section, India



Fig. 2.23 *Left* verging folded quartz veins with hinge zones much thicker than the limbs. Its axial trace sub-parallel the foliation, therefore the vergence cannot be used reliably as a shear sense indicator. Instead, a train of quartz vein with sheared sigmoid bulges at right gives a *top-to-left (up)* shear sense. *Location* Greater Himalayan Crystallines, Bhagirathi section, India

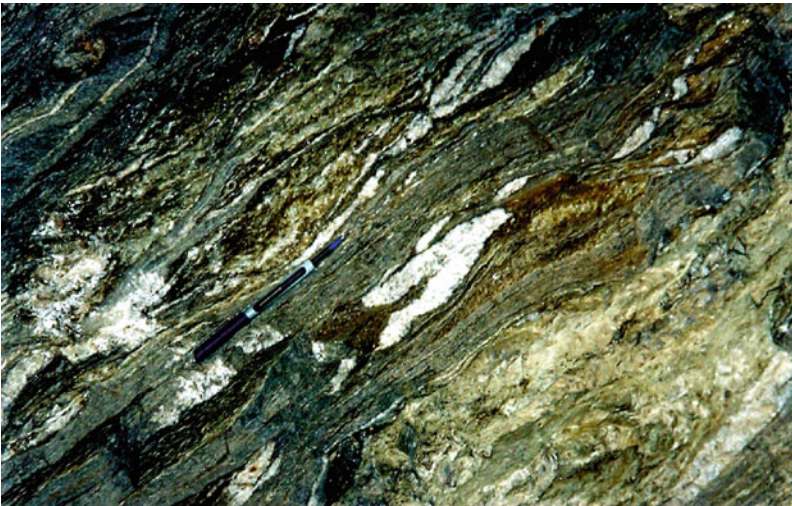


Fig. 2.24 *Right* to the marker (pen), a rootless flame fold of quartz with axial trace parallel to the *left* dipping mylonitic foliation. The fold does not indicate any shear sense. However, a few sigmoid quartz mylonite pods interconnected by secondary synthetic ductile shear C' planes indicate reliably a *top-to-right (up)* shear, at top right portion of the photo. From mylonitized gneiss/migmatite of Greater Himalayan Crystallines, Sutlej section, India

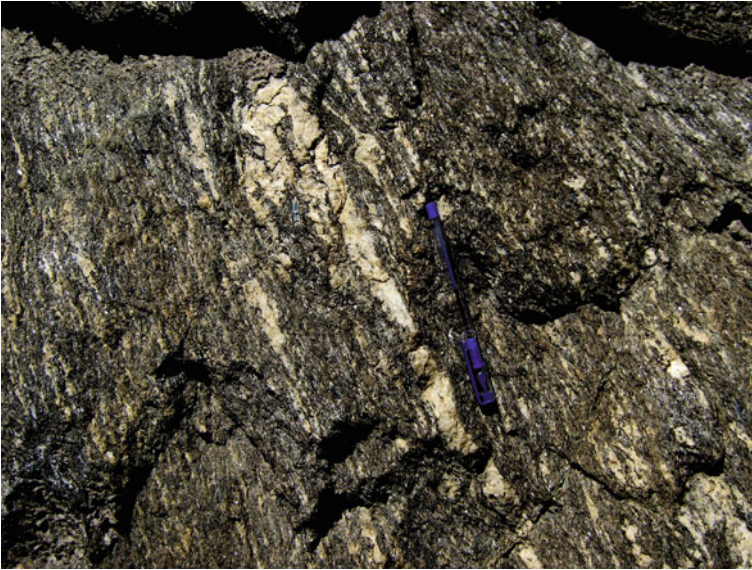


Fig. 2.25 A thicker quartz vein of irregular margins is folded isoclinally and is bound by migmatitic/gneissic foliations. The axial trace of this intrafolial fold sub-parallel the foliation.
Location Greater Himalayan Crystallines, Bhagirathi section, India



Fig. 2.26 A sheath fold from migmatized gneiss from Greater Himalayan Crystallines, Bhagirathi section (India). These folds were considered by previous workers as indicators of high strain. See Reber et al. (2013) as a latest work on sheath folds



Fig. 2.27 A sheath fold from migmatized gneiss from Greater Himalayan Crystallines, Bhagirathi section (India). Curvature/closure of limb is seen especially at *top left* corner of the fold. Does asymmetry of sheath folds also indicate (here a *top-to-left*) shear sense? Interestingly, Dell et al. (2013) analogue modeled development of sheath fold during progressive shear



Fig. 2.28 An overturned intrafolial fold of gneissic foliation with a rightward vergence. *Top-to-right* (*up*) shear. The fold is bound at *top* by nearly *straight* foliations. *Location* Greater Himalayan Crystallines, Sutlej section (India)



Fig. 2.29 Neutral folded psammitic schist with M-geometry in the hinge zone. *Location* Tethyan Himalaya, near Jangi check post. Sutlej section (India)



Fig. 2.30 Zeolite vesicles within Deccan basalt at Malsejghat, Maharashtra. In first appearance, a single vesicle appears to get isoclinally folded. Hinge thicker than the limbs. However, these structures are produced due to escape of gas bubble upwards when the lava (now the country rock) was hot, and subsequent coalescence of the bubbles. Zeolite later filled up the vesicles



Fig. 2.31 Same interpretation as the previous Fig. 2.30. Deccan trap basalt at Malsejghat, Maharashtra



Fig. 2.32 Elongated zeolite vesicles plunging towards *right*. A few appear folded. Same interpretation as that for Fig. 2.30. Deccan trap basalt at Malsejghat. Maharashtra



Fig. 2.33 A train of isoclinal round hinge folds of granitic material that came out from the margin of a dyke. These folds are *not* ductile shear sense indicators. Ambaji, Gujarat, India

References

- Alsop GI, Holdsworth RE (2004) Shear zone folds: records of flow perturbation or structural inheritance? In: Alsop GI, Holdsworth RE, McCaffey KJW, Hand M (eds) Flow processes in faults and shear zones. Geol Soc London 224:177–199 (Special Publications)
- Beaumont C, Jamieson RA (2010) Himalayan–Tibetan Orogeny: channel flow versus (critical) wedge models, a false dichotomy? In: Leech ML et al (eds) Proceedings for the 25th Himalaya–Karakoram–Tibet workshop: U.S. Geological Survey, Open-File Report
- Bell TH (2010) Deformation partitioning, foliation successions and their significance for orogenesis: hiding lengthy deformation histories in mylonites. In: Law RD, Butler RWH, Holdsworth RE, Krabbendam M, Strachan RA (eds) Continental tectonics and mountain building: the legacy of peach and Horne. Geol Soc London 335:275–292 (Special Publications)
- Dell D, Ertole, Schellart WP (2013) The development of sheath folds in viscously stratified materials in simple shear conditions: an analogue approach. J Struct Geol (in press)
- Klein C, Philpotts A (2013) Earth materials: introduction to mineralogy and petrology. Cambridge University Press, pp 419
- Mukherjee S (2010) Structures in Meso- and Micro-scales in the Sutlej section of the Higher Himalayan Shear Zone, Indian Himalaya. e-Terra 7:1–27
- Mukherjee S (2013a) Deformation microstructures in rocks. Springer, Berlin, pp 1–111
- Mukherjee S (2013b) Higher Himalaya in the Bhagirathi section (NW Himalaya, India): its structures, backthrusts and extrusion mechanism by both channel flow and critical taper mechanisms. Int J Earth Sci 102:1851–1870

- Mukherjee S, Ghosh R (2013) Both channel flow and critical taper operated on the Greater Himalayan crystallines (GHC)—a review. In: 28th Himalaya Karakoram Tibet workshop and 6th international symposium on Tibetan Plateau 2013. Tuebingen University, Germany
- Mukherjee S, Koyi HA (2010a) Higher Himalayan Shear Zone, Sutlej section: structural geology and extrusion mechanism by various combinations of simple shear, pure shear and channel flow in shifting modes. *Int J Earth Sci* 99:1267–1303
- Mukherjee S, Koyi HA (2010b) Higher Himalayan Shear Zone, Zaskar Indian Himalaya—microstructural studies and extrusion mechanism by a combination of simple shear and channel flow. *Int J Earth Sci* 99:1083–1110
- Mukherjee S, Puneekar JN, Mahadani T et al (2013) Intrafolial folds—review and examples from the western Indian Higher Himalaya. *Geol J* (Submitted)
- Reber JE, Dabrowski M, Galland O et al (2013) Sheath fold morphology in simple shear. *J Struct Geol* 53:15–26
- Wennberg OP (1996) Superimposed fabric due to reversal of shear sense: an example from the Bergen Arc Shear Zone, western Norway. *J Struct Geol* 18:871–889

Chapter 3

Veins and Near Symmetric Clasts

Near symmetric clasts of quartz and feldspar have classically been described as augens (Figs. 3.1, 3.2, 3.3, 3.4, 3.5, 3.6, 3.7, 3.8, 3.9, 3.10, 3.11, 3.12, 3.13, 3.14, 3.15, 3.16, 3.17, 3.18, 3.19, 3.20, 3.21, 3.22, 3.23; Figs. 3.31, 3.32, 3.33, 3.34, 3.35), and have been neglected so far possibly because they are not useful in ductile shear sense determination. These clasts are commonly elliptical with their long axes sub-parallel to the shear planes (Figs. 3.1, 3.5, 3.6, 3.7, 3.17, 3.22, 3.26, 3.31, 3.32, 3.33), seldom rhombic (Figs. 3.2, 3.3, 3.4), and could be parts of veins (Fig. 3.1), get pinched and swelled (Figs. 3.13, 3.14, 3.16), or simply irregular-shaped (Figs. 3.8, 3.9, 3.10, 3.11, 3.12, 3.33, 3.34 and 3.35). On the other hand, quartz rich veins within ductile shear zones may run parallel to the ductile shear planes (Figs. 3.24, 3.25), or cut across them (Figs. 3.27, 3.28, 3.29, 3.30). In the later case, the veins may themselves be also ductile sheared (Figs. 3.27, 3.28, 3.30). Symmetric objects in ductile shear zones that do not decode shear sense has been exemplified under optical microscopes by many such as Passchier and Trouw (2005) and Mukherjee (2013a). Most of the photographs described in this section for symmetric clasts and unshared veins bear no tectonic connotations.



Fig. 3.1 A near-symmetric rhombic bulged part of a quartz vein. No clear ductile shear sense indicated. From mylonitized gneiss at Sutlej section of Greater Himalayan Crystallines, Himachal Pradesh, India. Reproduced from Fig. 3b of Mukherjee (2010). Such feature in micro-scale were presented in Mukherjee (2013a)



Fig. 3.2 A near-rhombic clast of quartz with all the margins curved. Being symmetric, no ductile shear sense is indicated. Location: Greater Himalayan Crystallines, Bhagirathi section, India. See Mukherjee (2013b) for a latest review on tectonics of this terrain



Fig. 3.3 A symmetric rhombic ϕ -structure defined by an aggregate of quartzofeldspathic minerals. No shear sense indicated. From mylonitized gneiss at Bhagirathi section of Greater Himalayan Crystallines, India

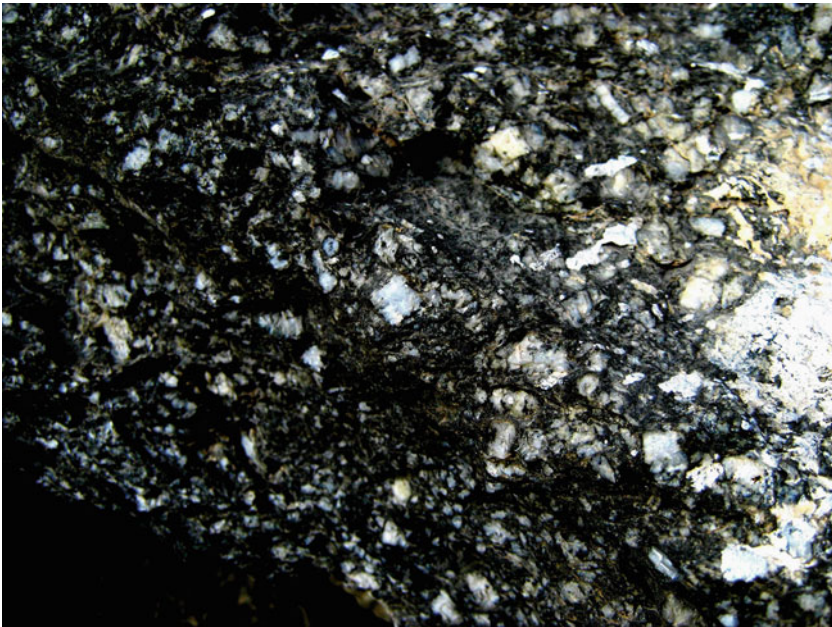


Fig. 3.4 Irregular feldspar clasts—a few rhombic, do not indicate any shear sense. Location: Greater Himalayan Crystallines, Bhagirathi section, India



Fig. 3.5 A rootless symmetric lenticular quartz vein with internal foliations parallel to the external ones within the host rock. No ductile shear sense indicated. Greater Himalayan Crystallines, Bhagirathi section, India



Fig. 3.6 A rootless symmetric lenticular quartz vein with internal foliations parallel to the external ones within the host rock. No ductile shear sense indicated. Greater Himalayan Crystallines, Bhagirathi section, India

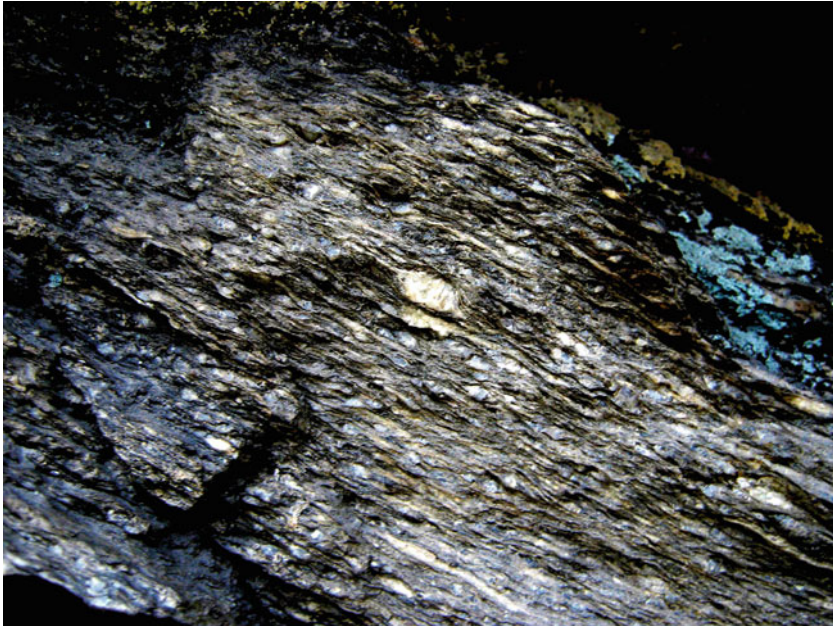


Fig. 3.7 A mylonitized augen gneiss. The biggest clast here is lenticular, symmetric and has tails. No shear sense indicated. Location: Greater Himalayan Crystallines, Bhagirathi section, India



Fig. 3.8 Irregular feldspar clasts, do not indicate any shear sense. Location: Greater Himalayan Crystallines, Bhagirathi section, India



Fig. 3.9 Irregular feldspar clasts, do not indicate any shear sense. Location: Greater Himalayan Crystallines, Bhagirathi section, India

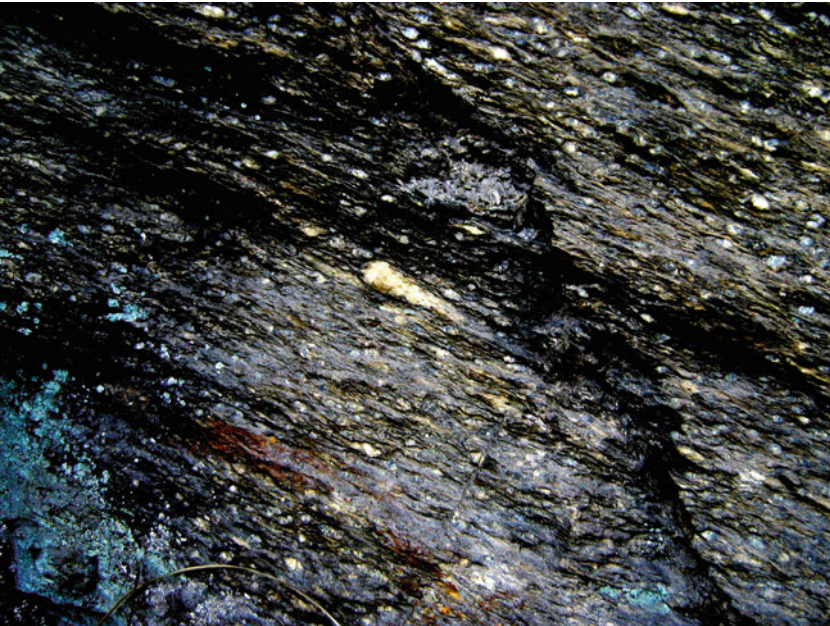


Fig. 3.10 Elongated clast of quartz parallel to the main foliation. No shear sense indicated. Location: Greater Himalayan Crystallines, Bhagirathi section, India



Fig. 3.11 Inside anastomosed foliated ductile sheared rock, symmetric clasts of rather irregular shapes persist. These were previously described as 'augen' structures. From mylonitized gneiss at Bhagirathi section of Greater Himalayan Crystallines, India



Fig. 3.12 An irregular clast of quartz with tails at two sides. No clear-cut ductile shear sense indicated. From mylonitized gneiss at Bhagirathi section of Greater Himalayan Crystallines, India



Fig. 3.13 Nearly symmetric and a little pinched centrally clast of quartz along with tails of different lengths. No ductile shear sense indicated. At immediate *left* and also *above, top-to-left* sheared clasts. Location: Greater Himalayan Crystallines, Bhagirathi section, India



Fig. 3.14 Pinched and swelled quartz vein within mylonitized gneiss. Gneissosity warped near the pinch. Greater Himalayan Crystallines, Bhagirathi section, India

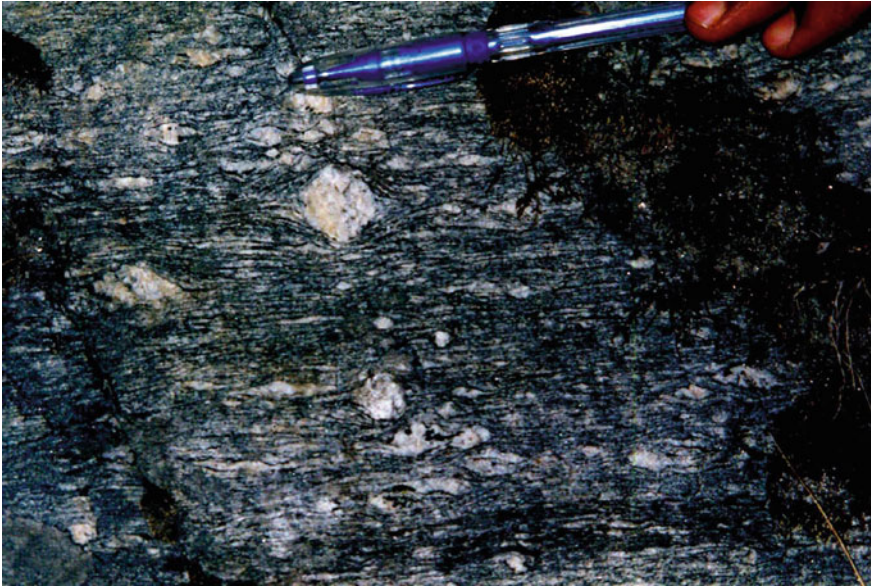


Fig. 3.15 A symmetric ϕ -object from mylonitized gneiss. *Tails* at two sides parallel the mylonitic foliation. No ductile shear sense indicated. Greater Himalayan Crystallines, Goriganga section, India



Fig. 3.16 An irregular clast of quartz that does not indicate any shear sense. Location: Greater Himalayan Crystallines, Bhagirathi section, India



Fig. 3.17 An augen gneiss/sheared mylonite with lenticular/subrounded clasts. No clear shear sense indicated since a number of clasts are not inclined consistently in a single direction with respect to the foliations that dip towards *right*. Location: Greater Himalayan Crystallines, Bhagirathi section, India

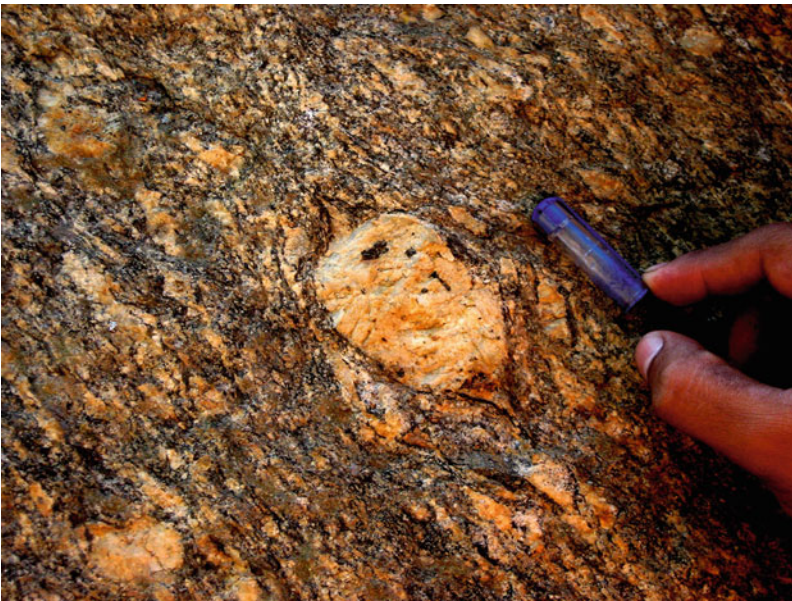


Fig. 3.18 A symmetric porphyroblast of feldspar with short tails. No shear sense indicated. The blast is selectively fractured near the margin. Location: Greater Himalayan Crystallines, Bhagirathi section, India



Fig. 3.19 A symmetric clast of feldspar with tail along the foliation, inside an augen gneiss/mylonitized gneiss. Greater Himalayan Crystallines, Bhagirathi section, India



Fig. 3.20 A nearly symmetric object (quartz) with tails sub-parallel to the mylonitic foliations. Greater Himalayan Crystallines, Bhagirathi section, India

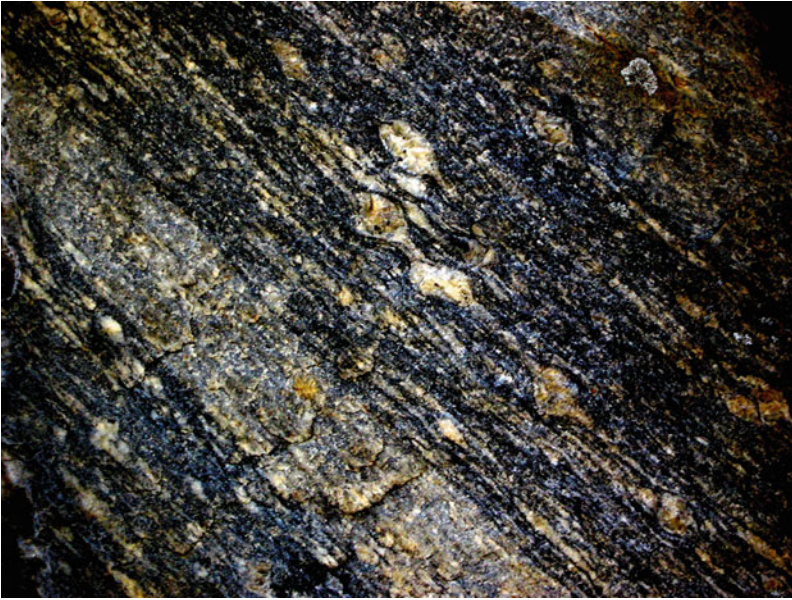


Fig. 3.21 Two adjacent feldspar clasts inside augengneiss/mylonitized gneiss. Shape asymmetry indicates reverse sense of shear. However, detail study of shape asymmetry of this rock is needed, preferably under an optical microscope, to confirm this. Location: Greater Himalayan Crystallines, Bhagirathi section, India



Fig. 3.22 A lenticular quartz porphyroblast. No shear sense indicated. A sigmoid clast at its *right bottom* is *top-to-left (up)* sheared. Location: Greater Himalayan Crystallines, Bhagirathi section, India

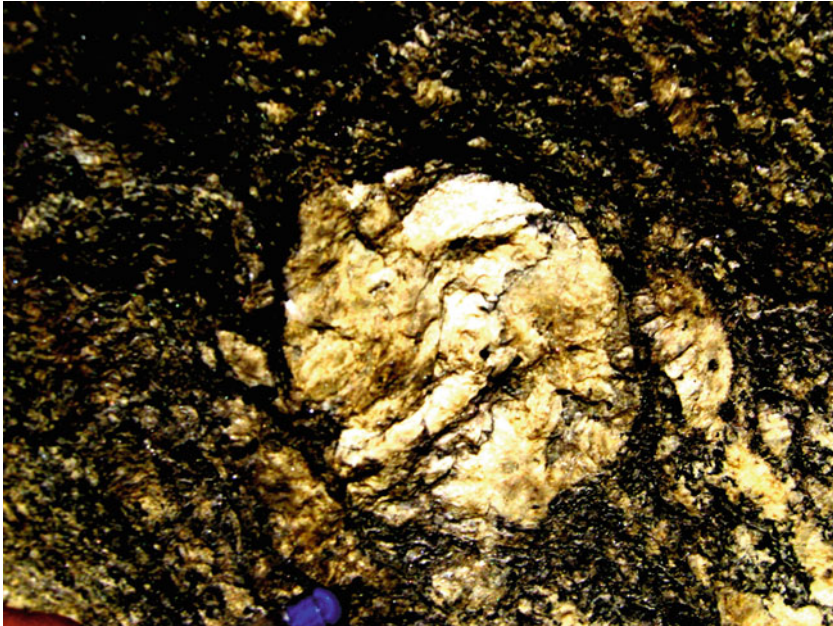


Fig. 3.23 A sub-rounded clast of weak asymmetry. No clear cut shear sense indicated. From mylonitized gneiss at Bhagirathi section of Greater Himalayan Crystallines, India



Fig. 3.24 A rootless quartz vein in a mica schist. Location: Greater Himalayan Crystallines, Bhagirathi section, India



Fig. 3.25 A rootless quartz vein within ductile shear zone attained nearly lenticular shape. No shear sense indicated. Location: Greater Himalayan Crystallines, Bhagirathi section, India



Fig. 3.26 Quartzofeldspathic layers at places swelled to symmetric lenticles. No ductile shear sense indicated. Location: Greater Himalayan Crystallines, Bhagirathi section, India. Fig. 15b of Simpson and De Paor (1993) reports a similar feature



Fig. 3.27 A quartz vein cut across the gneissic foliations. In addition, at several places along foliations, the quartz vein got sheared. Some parts of the sheared vein are sigmoidal and give a *top-to-left (up)* shear. This also matches with the sense displayed by sheared clasts at *top-left* portion of the photo. Note the topmost part of the vein is entirely sheared. Intrusion of the vein was either a pre- or a syn-shearing event. Greater Himalayan Crystallines, Bhagirathi section, India. Deformed and stretched cross-cutting elements were also reported in Fig. 3b of Maeder et al. (2009). Also see Maeder (2007)

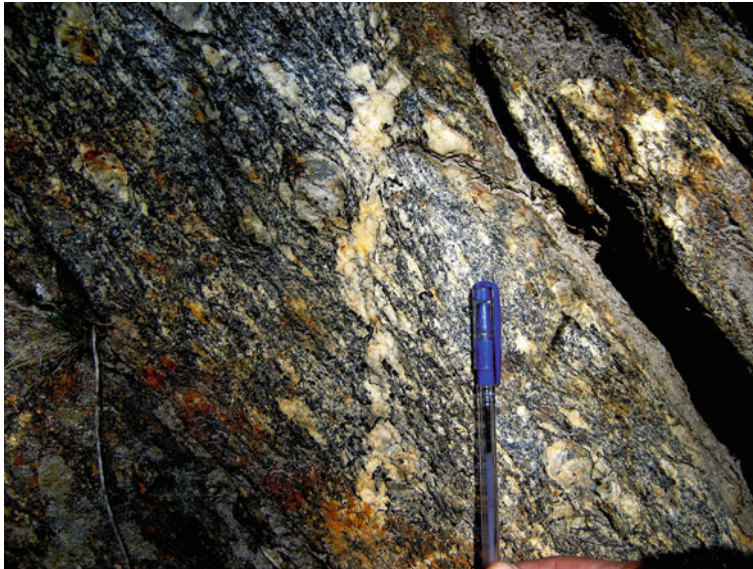


Fig. 3.28 Similar to the caption of Fig. 3.27. Intrusion of vein was certainly not a post-*top-to-left (up)* shearing event. Mylonitic foliations at places swerve strongly near the shear vein. Greater Himalayan Crystallines, Bhagirathi section, India. Reproduced from Fig. 19a of Mukherjee (2013c)

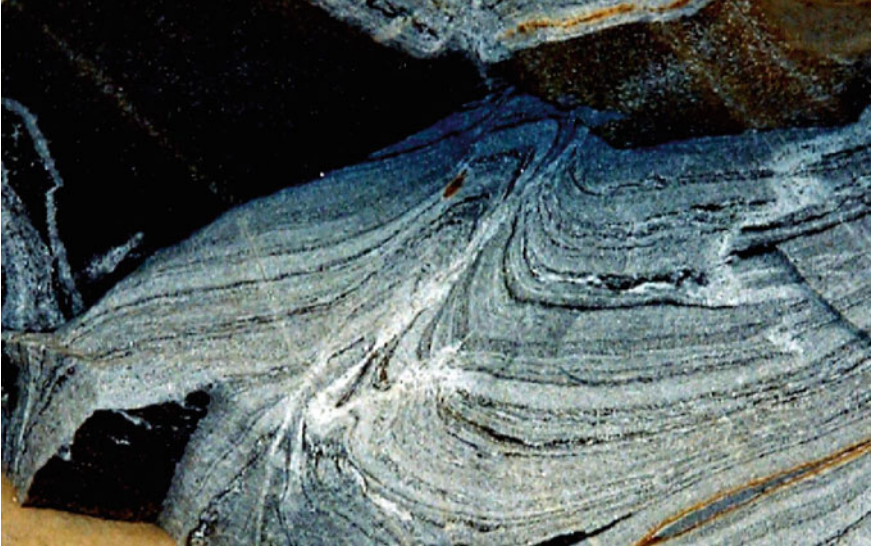


Fig. 3.29 Near cross-cutting element veins of quartz within migmatitic gneiss, the mylonitic foliations are strongly warped. Greater Himalayan Crystallines, Sutlej section, Himachal Pradesh, India. Reproduced from Fig. 18c of Mukherjee (2010)



Fig. 3.30 An overturned isoclinal fold of quartz vein (*left to the pen*), and a deformed vein of irregular geometry indicate possibly a *top-to-right* ductile shear. Ambaji, Gujrat, India. Reproduced from Fig. 19c of Mukherjee (2013c)



Fig. 3.31 A lenticular/rhombic quartz vein with long axis parallel to the main foliation inside mylonitized gneiss. No shear sense indicated. Location: Greater Himalayan Crystallines, Bhagirathi section, India



Fig. 3.32 A lenticular quartz vein inside ductile sheared mylonitized gneiss. Fractures at high angle to the main foliation developed inside the quartz lenticle. Location: Greater Himalayan Crystallines, Bhagirathi section, India



Fig. 3.33 An internally deformed irregular shaped clast from mylonitized gneiss at Bhagirathi section of Greater Himalayan Crystallines. The shape of the clast does not match with sigma-, delta- or phi-objects. No unambiguous shear sense indicated



Fig. 3.34 An internally deformed irregular shaped clast from mylonitized gneiss at Bhagirathi section of Greater Himalayan Crystallines. The shape of the clast does not match with sigma-, delta- or phi-objects. No unambiguous shear sense indicated. From mylonitized gneiss at Bhagirathi section of Greater Himalayan Crystallines



Fig. 3.35 A nearly lenticular clast with short straight margins. No clear ductile shear sense indicated. Mylonitic foliations dip towards *left*. From mylonitized gneiss at Bhagirathi section of Greater Himalayan Crystallines

References

- Maeder X (2007) The interaction of veins and foliations in metaturbidites of the lower Ugab Domain, NW Namibia. Ph.D. thesis. Johannes Gutenberg University of Mainz, pp 1–160
- Maeder X, Passchier CW, Koehn D (2009) Modelling of segment structures: boudins, bone-boudins, mullions and related single- and multiphase deformation features. *J Struct Geol* 31:817–830
- Mukherjee S (2010) Structures in meso- and micro-scales in the Sutlej section of the Higher Himalayan Shear Zone, Indian Himalaya. *e-Terra* 7:1–27
- Mukherjee S (2013a) Deformation microstructures in rocks. Springer, Berlin, pp 1–111
- Mukherjee S (2013b) Higher Himalaya in the Bhagirathi section (NW Himalaya, India): its structures, backthrusts and extrusion mechanism by both channel flow and critical taper mechanisms. *Int J Earth Sci* 102:1851–1870
- Mukherjee S (2013c) Review of flanking structures in meso- and micro-scales. *Geol Mag* (submitted)
- Passchier CW, Trouw RAJ (2005) *Microtectonics*, 2nd edn. Springer, Berlin
- Simpson C, De Paor DG (1993) Strain and kinematic analysis in general shear zones. *J Struct Geol* 15:1–20

Chapter 4

Boudins

Boudins are produced by local brittle-ductile extension in rocks. This collection presents pinch and swells (Figs. 4.8, 4.9, 4.10, 4.11, 4.17, 4.18, 4.20), foliation boudins (Figs. 4.5, 4.12, 4.16), shearband boudins (Figs. 4.3, 4.27), lenticular boudins (Figs. 4.2, 4.7, 4.15, 4.21, 4.22, 4.23, 4.24, 4.26), rare rotated boudins (Fig. 4.19), and trapezoid-shaped boudins (Fig. 4.25). Scar folds near the inter-boudin spaces most of the times have round hinges (such as Figs. 4.2, 4.7, 4.8, 4.9, 4.10, 4.15, 4.23). Asymmetric boudins were used as shear sense indicators (Goscombe et al. 2004; here Fig. 4.21). In some cases, the geometry of secondary quartz veins at the inter-boudin space matches with what has been described in the literature especially by Arslan et al. (2009a, b); see Figs. 4.1, 4.2, 4.3. In other cases, the quartz veins have diffuse margins (Figs. 4.6, 4.13, 4.14, 4.15) and do not possess regular geometries. Few boudins lack quartz veins at the inter-boudin space (Figs. 4.3, 4.7, 4.8, 4.9, 4.10, 4.11, 4.16, 4.17, 4.19, 4.20, 4.21, 4.22, 4.23, 4.25).

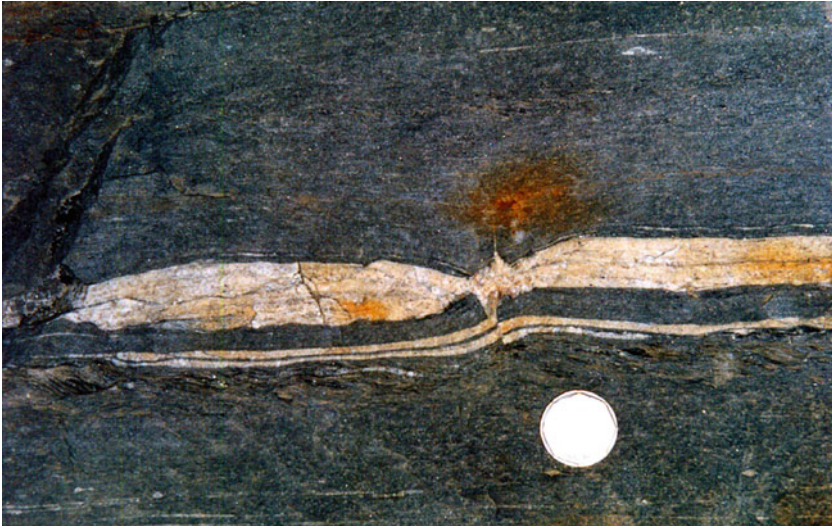


Fig. 4.1 Lenticular boudin of quartz vein. The inter-boudin space is occupied by *quadrilateral shaped* secondary quartz vein. The vein geometry matches with 'lozenge type' as described by Arslan et al. (2009a, b). This vein, prominent scar folds and the foliations within the matrix underwent a normal faulting. Ductile shear fabrics seen *below* the boudin. However, the sense of shear is difficult to comment conclusively. Goriganga section of Greater Himalayan Crystallines, India. Reproduced from Fig. 19d of Mukherjee (2013)



Fig. 4.2 A lenticular boudinaged calc-silicate layer within mylonitized gneiss/migmatite. Prominent round hinged scar folds. A pentagonal quartz deposition at the inter-boudin space. The vein geometry matches with 'X-type' as described by Arslan et al. (2009a, b). Near Karcham iron bridge, Sutlej section of Greater Himalayan Crystallines, Himachal Pradesh, India. Reproduced from Fig. 20a of Mukherjee (2013)



Fig. 4.3 A listric normal faulted calc-silicate layer within mylonitized gneiss/migmatite. Partly boudinaged calc-silicate layer shows internal foliations that parallel that within the host rock. Near Karcham iron bridge, Sutlej section of Greater Himalayan Crystallines, Himachal Pradesh, India. Reproduced from Fig. 20d of Mukherjee (2013)



Fig. 4.4 An irregular quartz body at the inter-boudin space. Migmatitic foliations within the host rock are prominently folded locally near the quartz body. Sutlej section of Greater Himalayan Crystallines, Himachal Pradesh, India

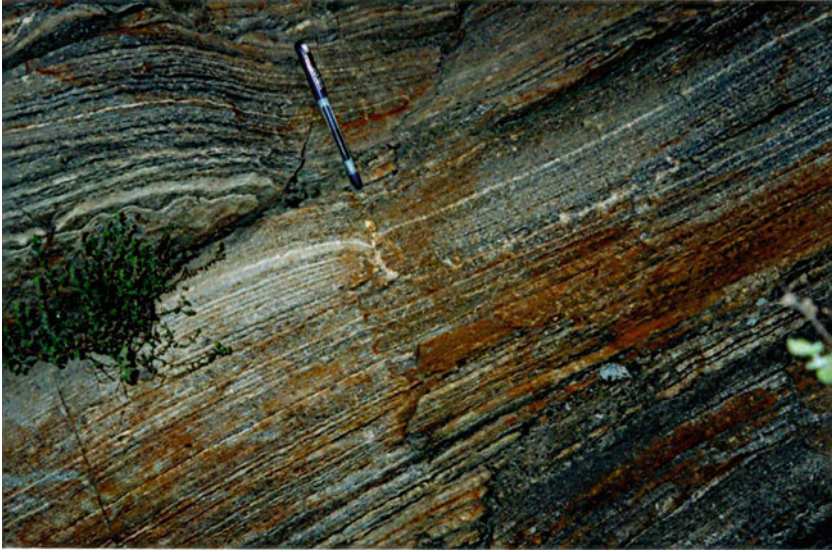


Fig. 4.5 Layered migmatitic gneiss shows foliation boudinage. A quartz vein convex towards left occupies the pinched part of the boudin. The vein geometry matches with ‘crescent type’ as described by Arslan et al. (2009a, b). Greater Himalayan Crystallines, Himachal Pradesh, India



Fig. 4.6 Inter-boudin space in a foliation boudin inside a migmatitic gneiss is occupied by secondary quartz of irregular geometry. Prominent scar folds of sub-rounded hinges. Location near an unnamed iron bridge near Karcham, Greater Himalayan Crystallines in Sutlej section, India



Fig. 4.7 Symmetric lenticular boudins of quartz within gneiss of the Greater Himalayan Crystallines at Dhauliganga section, India. Notice close spaced biotite foliations bound these boudis and also occupy the inter-boudin space



Fig. 4.8 A pinch and swell structure of quartz vein. Prominent scar folds. Hammer for marker. *Location* Powari, Greater Himalayan Crystallines in Sutlej section, Himachal Pradesh, India. Reproduced from Fig. 10c of Mukherjee and Koyi (2010)



Fig. 4.9 Pinched and swelled foliations. Greater Himalayan Crystallines at Goriganga section, India



Fig. 4.10 Pinch and swell structure of calc-silicate layer within mylonitized gneiss. Foliations within the boudin sub-parallel that within the host rock. Greater Himalayan Crystallines at Sutlej section, Himachal Pradesh, India



Fig. 4.11 Multiply pinched quartz vein (*above the coin*) within gneiss. Ambaji, Gujarat, India

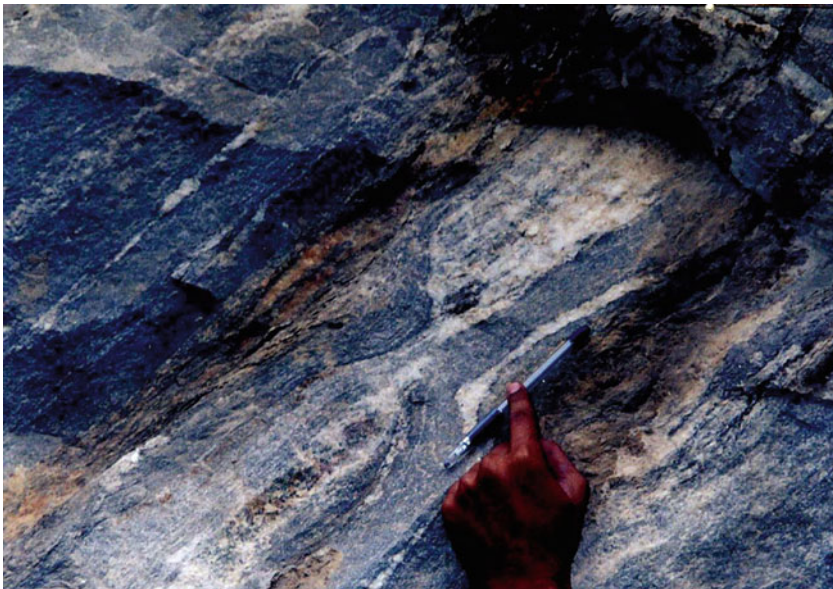


Fig. 4.12 Foliation boudins. The *left bottom* boudin is more *lenticular shaped*. Prominent round hinge scar fold of foliation and a quartz vein at the pinch. At *top left corner*, foliations show dip towards *left*. Near Karcham hydropower plant, Sutlej section of Greater Himalayan Crystallines. Himachal Pradesh, India



Fig. 4.13 A boudinaged calc-silicate layer along the *left* dipping foliation plane shows accumulation of quartz as a polygon at the inter-boudin space. Scar folds more prominent at bottom. A second minor pinch is present *above* folded fingers. Near Karcham hydropower plant, Sutlej section of Greater Himalayan Crystallines. Himachal Pradesh, India. Reproduced from Fig. 20b, c of Mukherjee (2013)



Fig. 4.14 Similar caption as Fig. 4.13 except that scar folds are almost absent. Near Karcham hydropower plant, Sutlej section of Greater Himalayan Crystallines, India. Notice that even layer parallel extension (e.g. Figs. 7d,e of Abe and Ural 2012) and layer perpendicular compression (Figs. 9,10 of Komoróczy et al. 2013) can rotate few boudins



Fig. 4.15 Lenticular boudins of a calc-silicate layer. Prominent scar folds at inter-boudin space. Irregular quartz veins of different geometries at inter-boudin spaces. Sutlej section of Greater Himalayan Crystallines, Himachal Pradesh. Reproduced from Fig. 10a of Mukherjee and Koyi (2010)

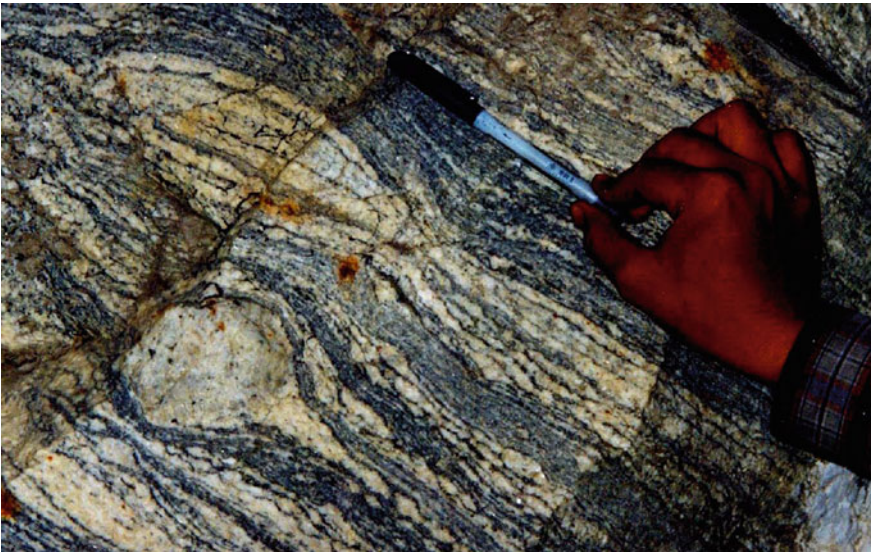


Fig. 4.16 Foliation boudinage within migmatite with *thicker* leucosomes and *thinner* melanosomes. An asymmetric pod of leucosome below the boudin. Sutlej section of Greater Himalayan Crystallines, Himachal Pradesh, India. Reproduced from Fig. 10d of Mukherjee and Koyi (2010)



Fig. 4.17 Pinch and swell structure from Fig. 10b of quartz within psamitic schist. Near Shongthong, Sutlej section of Greater Himalayan Crystallines, Himachal Pradesh. India. Reproduced from Fig. 10a of Mukherjee and Koyi (2010)

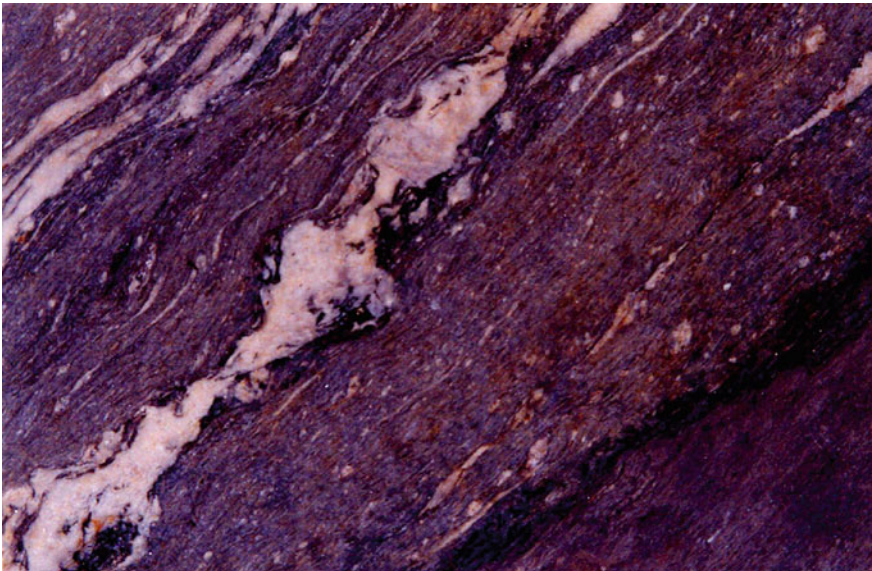


Fig. 4.18 Pinch and swelled quartz vein. The swelled portions are nearly symmetric and do not indicate any shear sense. The matrix foliations are warped. Dhauliganga section of Greater Himalayan Crystallines



Fig. 4.19 Rare rotated boudins within gneiss. Ambaji, Gujarat, India



Fig. 4.20 A part of a granite dyke got pinched and swelled (*below* the pen). Well developed scar folds. Ambaji, Gujarat, India



Fig. 4.21 *Top-to-right* ductile sheared quartz clasts/fish develop shearband boudins. The clasts are joined by 'tails'. Prominent scar folds of schistosity planes of the host rock. Ambaji, Gujarat, India



Fig. 4.22 A lenticular boudinaged clast of quartz. Prominent scar folded schistosity planes are cut by a fracture plane at high-angle to it (see *above* the quartz clast). Notice that the fracture is restricted within the host rock and does not pass through the clast. Ambaji, Gujarat, India



Fig. 4.23 Lenticular boudins of quartz clasts. Prominent scar folds—especially just *above* the finger. Ambaji, Gujarat, India



Fig. 4.24 A lenticular boudinaged quartz clast was cut-across by a sub-vertical fracture plane. Ambaji, Gujarat, India



Fig. 4.25 A folded and boudinaged granite dyke. The boudins are of trapezoidal geometry. See Sengupta (1983) for their genesis. Ambaji, Gujarat, India



Fig. 4.26 A warped dyke of granite pinched at places. A few fractures developed at *right angle* to the dyke margin and within the dyke. Ambaji, Gujarat, India



Fig. 4.27 A brittle faulted granite dyke. Finger indicates slip direction. Although the fault is absent in the host rock, it can be traced in an adjacent dike (*below*). Ambaji, Gujarat, India

References

- Abe S, Urai J (2012) Discrete element modeling of boudinage: insights on rock rheology, matrix flow, and evolution of geometry. *J Geophys Res* 117:B01407
- Arslan A, Koehn D, Passchier CW et al (2009a) The transition from single layer to foliation boudinage: a dynamic modeling approach. *J Struct Geol* 42:118–126
- Arslan A, Passchier CW, Koehn D (2009b) Foliation boudinage. *J Struct Geol* 30:291–309
- Goscombe BD, Passchier CW, Hand M (2004) Boudinage classification: end-member boudin types and modified boudin structures. *J Struct Geol* 26:739–763
- Komoróczy A, Abe S, Urai JL (2013) Meshless numerical modeling of brittle-viscous deformation: first results on boudinage and hydrofracturing using a couple of discrete element method (DEM) and smoothed particle hydrodynamics (SPH). *Comp Geosci* 17:373–390
- Mukherjee S, Koyi HA (2010) Higher Himalayan shear zone, Sutlej section: structural geology and extrusion mechanism by various combinations of simple shear, pure shear and channel flow in shifting modes. *Int J Earth Sci* 99:1267–1303
- Mukherjee S (2013) Review of flanking structures in meso- and micro-scales. *Geol Mag* (submitted)
- Sengupta S (1983) Folding of boudinaged layers. *J Struct Geol* 5:197–210

Chapter 5

Brittle Shear

This chapter presents morphologic variations of P- and Y-planes of brittle shear. The inclination of P-planes, usually sigmoid-shaped, is a reliable indicator of brittle shear sense. Such brittle shear can be quite pervasive in the rocks (Fig. 5.1). Alternately, they can affect only along narrow zones (Figs. 5.2, 5.3, 5.4, 5.7, 5.32). The P-planes vary in sizes quite drastically (compare Figs. 5.4, 5.5, 5.6, 5.8). The Y-planes can be *sub-horizontal* (e.g. Figs. 5.9, 5.10, 5.11, etc.). Brittle shear defined by Y- and P-planes may be associated with synthetic secondary Riedel shearing R' (see Passchier and Trouw 2005; Fig. 5.12). Isolated lenses of rocks (Fig. 5.15) could indicate brittle shear. Instead of bound by a pair of Y-planes, sometimes the P-planes are found to be bound by a single Y-plane (e.g. Figs. 5.16, 5.59, 5.62). P-planes restricted with a part of rock/quartz veins is a common phenomenon (Figs. 5.17, 5.18, 5.19). Geometries of thrust slices may vary (Figs. 5.20, 5.21, 5.22; 5.27). The P-planes might be curved only near the Y-planes (Fig. 5.23). Fracturing of thrust slices in different ways is noted (Figs. 5.24, 5.25, 5.26). Rare examples of P-planes not bound by any Y-planes were observed (Fig. 5.28). The Y-planes are mutually sub-parallel (Figs. 5.1, 5.4, 5.11, 5.14, 5.20, 5.21, 5.22, 5.24, 5.27, 5.29, 5.30, 5.31, 5.34, 5.35, 5.37, 5.38, 5.39, 5.41, 5.44, 5.45, 5.46, 5.50, 5.52, 5.53, 5.54, 5.55, 5.57, 5.63) and usually straight. However, non-parallel Y-planes exist rarely (Figs. 5.32, 5.64). Sigmoidal thrust slices and P-planes are most common (Figs. 5.1, 5.4, 5.5, 5.6, 5.9, 5.10, 5.11, 5.12, 5.13, 5.14, 5.15, 5.16, 5.17, 5.18, 5.19, 5.20, 5.21, 5.22, 5.23, 5.24, 5.25, 5.27, 5.29, 5.30, 5.31, 5.32, 5.35, 5.36, 5.38, 5.39, 5.42, 5.43, 5.44, 5.45, 5.46, 5.47, 5.48, 5.49, 5.50, 5.51, 5.52, 5.53, 5.54, 5.55, 5.56, 5.57, 5.58, 5.59, 5.60, 5.63, 5.64). However, rhombic varieties do exist (Fig. 5.41). Poorly developed P-planes presumably indicate weak shearing (Fig. 5.57). Weavy Y-planes do exist (Fig. 5.61). During brittle shear, the P-planes develop from the Y-planes and migrate in a curvilinear manner to join at the adjacent parallel Y-plane (Tchlenko 1970, summarized by Handy et al. 2007). A few other eye-catching brittle shear sense indicators such as V-pull apart structure (Fig. 5.66), small-scale brittle faults along veins (Figs. 5.67, 5.68, 5.69), slickensides with peaks (Figs. 5.70, 5.71, 5.72). Brittle fractures not bound by sets of other fracture planes should not be related to brittle shear (Fig. 5.73). Greater Himalayan Crystallines in western Himalaya shows a top-to-S/SW fore-thrusting. However, backthrusting of top-to-N/NE sense has recently been reported from the Bhagirathi section (Mukherjee 2013) (Figs. 5.28, 5.29). The Y-plane can be sharp (Figs. 5.33, 5.40, 5.65).



Fig. 5.1 *Top-to-left (up)* brittle sheared gneisses of Bhagirathi section of the Greater Himalayan Crystallines. The Y-planes of brittle shear are longer, more straight and gentler than the P-planes. Both the Y- and the P-planes dip towards *right*. *Perpendicular* distances between adjacent Y-planes vary significantly. The P-planes are sigmoid-shaped and are bound by the Y-planes. No straight secondary brittle shear planes oblique to the Y-planes are noted. See Mukherjee (2013) for latest review on geology and tectonics of Bhagirathi section of the Greater Himalayan Crystallines, India



Fig. 5.2 A rather narrow zone of *top-to-left (up)* brittle sheared mylonitized gneiss (Bhagirathi section of the Greater Himalayan Crystallines, India). The shear is restricted where Arpan Bandyopadhyay put his hand



Fig. 5.3 *Top-to-left (up)* brittle sheared patch of quartzose body. Curved P-planes developed both inside and outside (especially at *top left* part) of the body at an angle to the Y-plane. At left to this body, a sheared vein of sigmoid bulge of same sense is also present. Greater Himalayan Crystallines, Bhagirathi section (India)



Fig. 5.4 *Top-to-right (up)* brittle sheared mylonitized gneiss. The shear is restricted within the two parallel Y-planes where Arpan Bandyopadhyay kept his hand. P-planes are confined within this layer, and cannot be found prominently in the surrounding rock. Greater Himalayan Crystallines, Bhagirathi section (India)

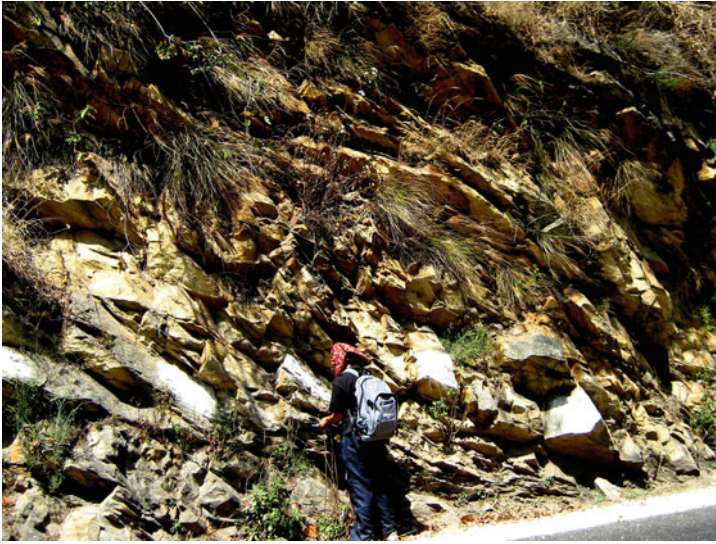


Fig. 5.5 *Top-to-left* sheared near sigmoid thrust slice with several sets of fractures. Location: Greater Himalayan Crystallines, Bhagirathi section (India)

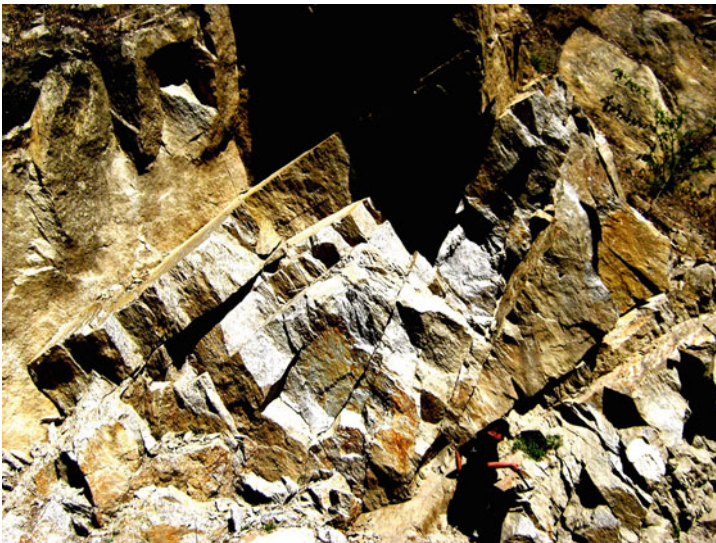


Fig. 5.6 *Top-to-right* brittle sheared mylonitized gneiss. Curved P-planes at one place define a sigmoid mass (just above the geologist marker). No Y-planes visible. Greater Himalayan Crystallines, Bhagirathi section (India)



Fig. 5.7 *Top-to-right (up)* brittle sheared mylonitized gneiss. A single prominent Y-plane (= brittle reverse fault plane) dips towards left. No other Y-plane is seen that could bound the P-planes at the other side. The curved P-planes are restricted only near the Y-plane. Greater Himalayan Crystallines, Bhagirathi section (India)



Fig. 5.8 *Top-to-left (up)* sheared gneiss of the Greater Himalayan Crystallines, Bhagirathi section (India). Dip directions of both the P and the Y-planes are the same (*towards left*). Reproduced from Fig. 6c of Mukherjee (2013)



Fig. 5.9 *Top-to-left* sheared gneiss of the Greater Himalayan Crystallines, Bhagirathi section (India). Note that the Y-planes that bound the *curved* P-planes are non-parallel



Fig. 5.10 *Top-to-left (up)* brittle sheared gneisses. Sujoy Kanti Ghosh as marker. Greater Himalayan Crystallines, Sutlej section, Himachal Pradesh, India



Fig. 5.11 *Top-to-right* sheared thrust slices (P-planes) bound by near parallel brittle shear Y-planes. Greater Himalayan Crystallines, Sutlej section, Himachal Pradesh, India



Fig. 5.12 *Top-to-right* brittle shear evident from quite a distance. Sigmoid thrust slices and fractures inside them define curved P-planes. The Y-plane of shear is weavy. Near the central portion of the photograph, a synthetic brittle shear plane R' is visible. Near Kharo bridge, Greater Himalayan Crystallines, Sutlej section, Himachal Pradesh, India. Reproduced from Fig. 11d of Mukherjee and Koyi (2010)



Fig. 5.13 *Top-to-right* sheared (sigmoid) thrust slices. Although snapped from a great distance, the Y-plane of brittle shear is still decipherable. Vegetations mask partly the sheared rock units. Greater Himalayan Crystallines, Sutlej section, Himachal Pradesh, India



Fig. 5.14 *Top-to-left (up)* sheared thrust slices overall defining a parallelogram shaped lens. Hammer for marker. An irregular black layer bounds this lens and might be a manifestation of shear heating of the country rock. Greater Himalayan Crystallines, Sutlej section, Himachal Pradesh, India



Fig. 5.15 An isolated sigmoid thrust slice defines the P-planes of brittle shear. *Top-to-left (up)* brittle sheared. *Right* to this slice, mylonitic foliation along with a few thicker white quartzofeldspathic layers of the ductile sheared gneiss also reveal S-fabrics and a *top-to-left (up)* ductile shear. Thus, the shear senses in the ductile and that in the brittle regime match. Greater Himalayan Crystallines, Sutlej section, Himachal Pradesh, India. Reproduced from Fig. 11c of Mukherjee and Koyi (2010)



Fig. 5.16 *Top-to-left (up)* sheared P-planes is bound by irregular Y-planes. The Y-plane in bottom is longer than that at top. Reproduced from Fig. 6b of Mukherjee (2013). Greater Himalayan Crystallines, Bhagirathi section, India



Fig. 5.17 Short nearly straight P-planes developed but those do not reach upto the Y-planes. *Top-to-left* shear. A single P-plane at right shows stepping. Mylonitized gneiss in Greater Himalayan Crystallines, Bhagirathi section, India



Fig. 5.18 A rootless quartz pod of irregular geometry within mylonitized schist shows *curved* sub-parallel fractures restricted solely inside the pod. *Top-to-right (up)* brittle shear. Greater Himalayan Crystallines, Bhagirathi section, India



Fig. 5.19 *Top-to-left* sheared P-planes restricted within a quartz pod inside mylonitized gneiss. Greater Himalayan Crystallines, Bhagirathi section, India



Fig. 5.20 *Top-to-left (up)* sheared P planes with significantly different curvatures. Mylonitized gneiss in Greater Himalayan Crystallines, Bhagirathi section, India



Fig. 5.21 *Top-to-right (up)* brittle shear displayed by sigmoid P-planes bound by Y-planes. Exact geometries of individual P-planes do not match. Both the P- and the Y-planes dip towards *left*. On the other hand, gneissic foliations dip towards right. Greater Himalayan Crystallines, Bhagirathi section, India. Reproduced from Fig. 8c of Mukherjee (2013)



Fig. 5.22 A *top-to-left (up)* brittle shear indicated by P-planes, a few of which are curved, bound by Y-planes. Angles between the Y and the P plane vary in adjacent cases. Greater Himalayan Crystallines, Bhagirathi section, India



Fig. 5.23 *Top-to-left (up)* brittle sheared P-planes within mylonitized gneiss of Greater Himalayan Crystallines at Bhagirathi section, India. The Y-plane is developed more prominently at top. Both the Y- and the P-planes dip towards right

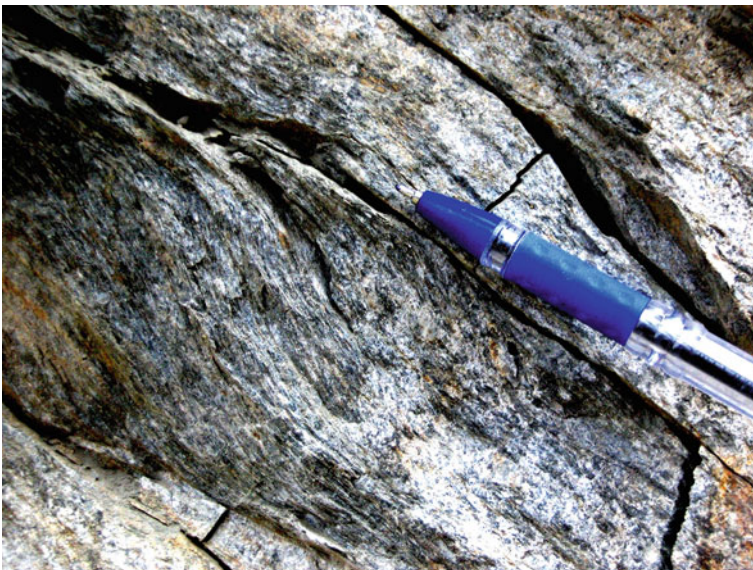


Fig. 5.24 S-C fabric mylonitized gneiss shows a *top-to-left (up)* ductile shear. Brittle P-plane parallel to the S-planes developed (indicating a *top-to-left* up brittle shear) possibly after the ductile deformation. The brittle Y-plane parallels the ductile C-plane. Greater Himalayan Crystallines, Bhagirathi section, India



Fig. 5.25 A *top-to-left* brittle sheared quartz vein within weakly ductile sheared gneiss, near Ambaji temple, Ambaji, Gujarat. The thrust slice was multiply fractured



Fig. 5.26 *Top-to-left (up)* sheared quartz vein that later got fractured at an angle to the Y-plane. Greater Himalayan Crystallines, Sutlej section, Himachal Pradesh, India

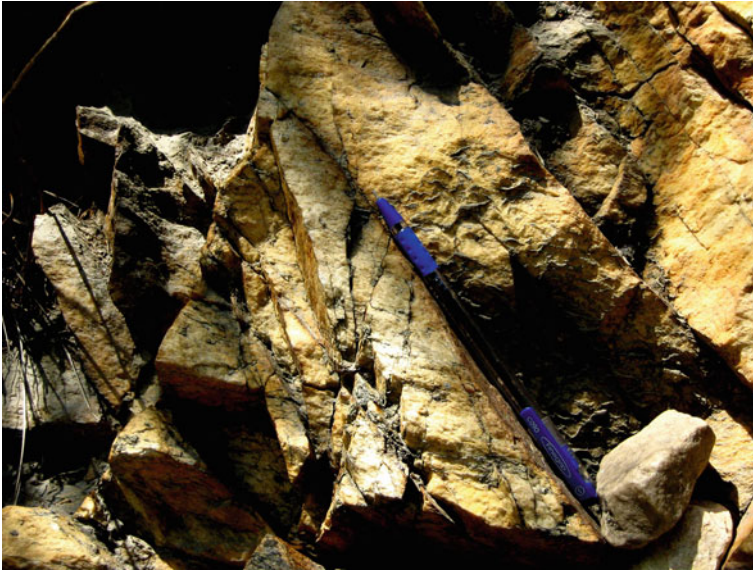


Fig. 5.27 *Top-to-left (up)* sheared Gangotri Granite, Greater Himalayan Crystallines, Bhagirathi section (India). Non-parallel straight P-planes are bound by straight Y-planes. P-planes are not developed right to the pen. Reproduced from Fig. 12b of Mukherjee (2013)



Fig. 5.28 *Top-to-right (up)* brittle sheared brittle P-planes. No sharp/clear Y-planes are present. These P-planes do not resemble their usual curvature (e.g. Fig. 5.6). The P-planes dip towards right at a steeper angle than the gneissic foliation planes. Greater Himalayan Crystallines, Bhagirathi section (India). Reproduced from Fig. 8c of Mukherjee (2013)



Fig. 5.29 *Top-to-right (up)* brittle sheared *curved* P-planes are bound by much straight and parallel Y-planes. Notice that curvatures of the P-planes are not like their usual appearances (e.g. Fig. 5.6). Both the P- and the Y-planes dip towards *left*, whereas the gneissic foliations towards *right*. Greater Himalayan Crystallines, Bhagirathi section (India). Reproduced from Fig. 8d of Mukherjee (2013)



Fig. 5.30 *Top-to-right (down)* sheared thrust slices bound by sharp Y-planes (= brittle fault planes). Greater Himalayan Crystallines, Bhagirathi section (India)



Fig. 5.31 *Top-to-left (down)* brittle sheared psammitic schist. The Y-planes dip steeply. The P-planes run parallel although they are *curved*. Tethyan Himalaya, Sutlej section, Himachal Pradesh, India



Fig. 5.32 *Top-to-left (up)* brittle sheared P-planes within Siwalik rocks at Dehradun–Mussourie road. The P-planes are nearly straight. Notice that the brittle Y-planes are *curved* and are non-parallel. The P-planes are restricted inside the Y-planes. The Y-planes dip towards *right*, and the P-planes towards *left*



Fig. 5.33 *Top-to-left (up)* brittle sheared shorter nearly straight P-planes bound by sub-parallel Y-planes. The P-planes dip at steeper angles towards *right* than the Y-planes. Main Boundary Thrust Zone, Sahinsahi Ashram, near Dehradun, India



Fig. 5.34 A *left* dipping brittle fault zone within mylonitized gneiss. Fracture planes restricted inside it are sub-parallel. Therefore, the brittle shear sense cannot be deciphered. Bhagirathi section of Greater Himalayan Crystallines, India



Fig. 5.35 *Top-to-left (up)* brittle shear revealed by sigmoidal thrust slices of various sizes. These slices define the P-planes. From mylonitized gneiss at Sutlej section of Greater Himalayan Crystallines, Himachal Pradesh, India. Reproduced from Fig. 11b of Mukherjee and Koyi (2010)



Fig. 5.36 *Top-to-left (down)* brittle sheared psamitic schist. Not all near sigmoid P-planes are pervasive. The P-planes are *curved* only at their contacts with the Y-planes. Tethyan Himalaya, Sutlej section, Himachal Pradesh, India



Fig. 5.37 *Top-to-right (up)* brittle sheared P-planes restricted within irregular Y-planes. Notice that the P-planes are developed only at the central portion of the photograph. Both the P- and the Y-planes dip toward *left*. The P-planes dip steeper than the Y-planes. Bhagirathi section of Greater Himalayan Crystallines, India



Fig. 5.38 *Top-to-right (up)* sheared mylonitized gneiss. Sigmoid P-planes dip steeper than the more straight Y-planes. Both the P- and the Y-planes dip towards *right*. The Y-planes are more close spaced at top left than the central part of the photo. Bhagirathi section of Greater Himalayan Crystallines, India



Fig. 5.39 Sigmoid P-planes of migmatitic host rock bound by *sub-horizontal* Y-planes define a top-to-left shear. At right, a quartz vein also underwent the same shear. Notice that left to the hammer, no P-planes are developed. This means that portion of the rock escaped shearing. Greater Himalayan Crystallines, Sutlej section, Himachal Pradesh, India



Fig. 5.40 A *sub-horizontal* brittle fault plane inside mylonitized gneiss. Presuming folds adjacent to this fault to be due to a normal drag (such as Fig. 1 of Grasmann et al. 2003), a *top-to-left* slip is deduced. Alternately, the fault plane developed after folding. Greater Himalayan Crystallines, Bhagirathi section (India)



Fig. 5.41 Three parallelogram/rhombic thrust slices bound at *top* by *sub-horizontal* Y-planes near the central part of the photo. *Top-to-left* brittle sheared. Greater Himalayan Crystallines, Bhagirathi section (India)



Fig. 5.42 *Top-to-right* brittle sheared mylonitized gneiss. The P-planes are curved only near the Y-plane. The P-planes dip steeply towards *left*. Greater Himalayan Crystallines, Bhagirathi section (India)



Fig. 5.43 A *sub-vertical* fault plane deciphered from opposite senses of drag of foliations and fracture planes *across* it. The shear sense is shown by a half *arrow*. Fracture planes near the fault plane seemed to form due to faulting. Gangotri Granite. Greater Himalayan Crystallines, Bhagirathi section (India)



Fig. 5.44 Black 'burnt rock' (Mukherjee 2013) shows *top-to-right (up)* brittle shear. *Curved* P-planes bound by *sub-parallel* left dipping Y-planes. Greater Himalayan Crystallines, Bhagirathi section (India). Similar to Fig. 10b of Mukherjee (2013)



Fig. 5.45 *Top-to-right* brittle sheared P-planes. Two trains of P-planes are seen. The Y-plane is best developed at the *bottom* part of the photograph. Notice that at right extremity of the photograph, the P-planes are difficult to decipher. Greater Himalayan Crystallines, Bhagirathi section (India). Similar to Fig. 10b of Mukherjee (2013)



Fig. 5.46 *Top-to-right (down)* brittle sheared Gangotri Granite. The P-planes are obscure at places but are still decipherable. The Y-planes dip towards *right*, and the P-planes towards *left*. Bhagirathi section of Greater Himalayan Crystallines, India. Similar to Fig. 11a of Mukherjee (2013)



Fig. 5.47 *Top-to-right (down)* brittle sheared Gangotri Granite. Notice the P-planes are step-like. Bhagirathi section of Greater Himalayan Crystallines, India



Fig. 5.48 *Top-to-right (up)* brittle sheared P-planes. No Y-planes within the field of view that bound the P-planes. Bhagirathi section of Greater Himalayan Crystallines, India



Fig. 5.49 *Top-to-left (down)* brittle sheared curved P-planes restricted near a single Y-plane. Gangotri Granite at Bhagirathi section of Greater Himalayan Crystallines, India. Reproduced from Fig. 11c of Mukherjee (2013)



Fig. 5.50 *Top-to-left (down)* brittle sheared curved P-planes. Bothe the Y- and the P-planes dip towards *right*. Gangotri Granite at Bhagirathi section of Greater Himalayan Crystallines, India. Reproduced from Fig. 11c of Mukherjee (2013)



Fig. 5.51 *Top-to-left (down)* sheared granite where the P-planes are developed imperfectly. The Y-plane, however, is better developed. From Gangotri Granite, Greater Himalayan Crystallines, Bhagirathi section (India). Reproduced from Fig. 11d of Mukherjee (2013)



Fig. 5.52 *Top-to-left (down)* sheared P-planes affected quartz rich layers. From Gangotri Granite, Greater Himalayan Crystallines, Bhagirathi section (India). Reproduced from Fig. 12a of Mukherjee (2013)



Fig. 5.53 *Top-to-right (up)* brittle sheared Gangotri Granite. Both the P- and the Y-planes dip towards *left*. Greater Himalayan Crystallines, Bhagirathi section (India)



Fig. 5.54 *Top-to-right (up)* brittle sheared Gangotri Granite. The P-planes are strongly sigmoidal. Both the P- and the Y-planes dip towards *left*. Reproduced from Fig. 12c of Mukherjee (2013). Greater Himalayan Crystallines, Bhagirathi section (India)



Fig. 5.55 *Top-to-right (up) sheared P-planes dipping left are bound by brittle shear Y-planes dip in the same direction. Note the P-planes are quite irregular. From Gangotri Granite, Greater Himalayan Crystallines, Bhagirathi section (India)*



Fig. 5.56 *Top-to-right sheared P-planes bound by sub-horizontal Y-planes. This remains the first ever report of brittle shear from this terrain. Deccan trap basalt, near the MTDC guest house, Malsejghat. Maharashtra*



Fig. 5.57 Poorly developed concave rightward P-planes bound by *sub-horizontal* Y-planes. P-planes are usually sigmoid. Unlike that, the P-planes shown here are *curved* uniformly at one side. The Y-planes developed discontinuously at *top*. Deccan trap basalt, near the MTDC guest house, Malsejghat, Maharashtra



Fig. 5.58 Sigmoid P-planes bound at *top* by an irregular Y-plane demonstrate a *top-to-left* shear. No clear-cut Y-planes at *bottom* to the P-plane exist. Faint foliations restricted within the sheared bulge. These foliations terminate against the P-plane at *bottom*. Deccan trap basalt, near the MTDC guest house, Malsejghat, Maharashtra



Fig. 5.59 A single curved Y-plane bounds at *top* a set of P-planes that dip towards *left*. Deccan trap basalt, near the MTDC guest house, Malsejghat. Maharashtra



Fig. 5.60 *Top-to-right* sheared P brittle planes of sigmoid geometry. Notice that only at *bottom*, the Y-plane is developed that bound the P-planes, but not at the *top*. *Top-to-right* sheared. Located at the *vertical* exposure of basalts at the Mumbai-Pune expressway, Maharashtra, India



Fig. 5.61 Weavy *sub-horizontal* Y-plane bounds at a set of P brittle shear planes. The P-planes are very gently curved. *Top-to-left* brittle shear. An undulatory *sub-horizontal* brittle shear is typical of regional thrusting. However, this shear was not observed from any second exposure from the Kharghar hill. Basalts at Kharghat hill, Mumbai, Maharashtra, India. This shear sense was hitherto not reported from Mumbai nor from the Deccan basalts



Fig. 5.62 At the same location as that for Fig. 5.61, a *top-to-left* brittle shear is defined by gently curved P-planes dipping at *right* that terminates near a Y brittle plane. Note that this brittle shear zone near a Y plane is restricted within the *middle portion* of the photo, and does not persist in the *top part*. Basalts at Kharghat hill, Mumbai, Maharashtra, India



Fig. 5.63 A plan view. Whether this represents a *top-to-right* brittle shear in terms of *curved* P-planes bound by Y-planes cannot be said with certainty. Columnar joints of complicated geometry present in this area on plan might had produced such a geometry. From rhyolites of Aksa beach, Mumbai, Maharashtra



Fig. 5.64 In plan view, distinct curved planes of similar geometries bound by two planes confirm that the former are the P-planes, and the later are the Y-planes. *Top-to-right* sheared. From rhyolites of Aksa beach, Mumbai, Maharashtra. A number of such features with nearly the same ~northerly trend of Y-planes bring confidence in this interpretation



Fig. 5.65 In plan view, a set of brittle planes are found to be bound by another set of planes. At first it appears that the former are the P-planes, and the later are the Y-planes. However, these could be manifestation of columnar joints observed on plan. Columnar joints are abundant in this area. From rhyolites of Aksa beach, Mumbai, Maharashtra



Fig. 5.66 A V-pull apart structure of garnet within gneiss. *Top-to-left (up)* brittle sheared. Notice that the V is curved and the opening is filled up by quartz. This was probably the first ever report of such a structure from meso-scale. Location: North to Surraithota, Dhauliganga river section of Greater Himalayan Crystallines, western Indian Himalaya. Reproduced from Mukherjee (2010). For detail of V-pull aparts, consult Hippertt (1993), Singh (1996), Roy et al. (2010) etc



Fig. 5.67 A reverse faulted quartz vein within gneiss. Ambaji, Gujarat, India. No drag folds developed near the fault plane. Quartz vein also formed along the fault plane



Fig. 5.68 A reverse faulted quartz vein within gneiss. Ambaji, Gujarat, India. Quartz vein also formed along the fault plane



Fig. 5.69 A normal faulted quartz vein within gneiss. Ambaji, Gujarat, India



Fig. 5.70 A reverse fault plane with prominent slickensides and peaks. *Finger points* the direction of slip of the missing block. Greater Himalayan Crystallines at Bhagirathi section, India



Fig. 5.71 A fault plane with slickensides and peaks. The *pen points* the direction of slip of the missing block. Greater Himalayan Crystallines at Bhagirathi section, India

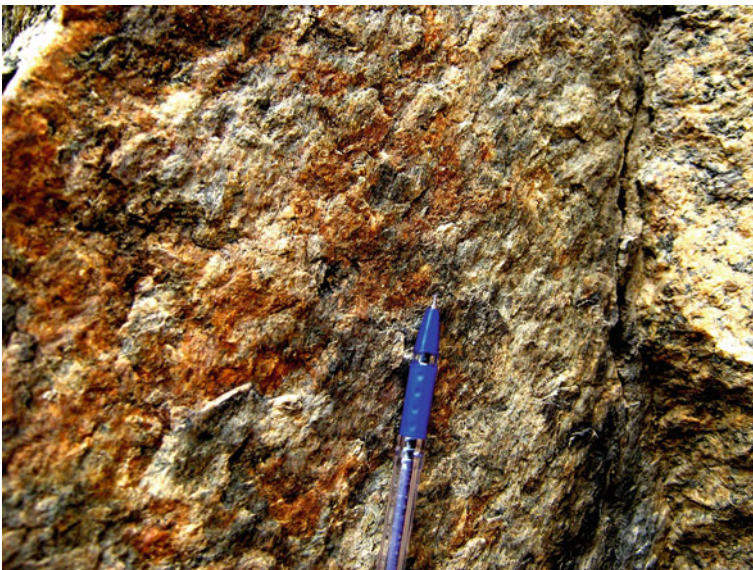


Fig. 5.72 A *sub-vertical* fault plane with prominent slickensides and peaks. The *pen points* the direction of slip of the missing block. Reproduced from Fig. 11b of Mukherjee (2013)



Fig. 5.73 Gently curved fractures. Ductile sheared gneiss within Greater Himalayan Crystallines, Bhagirathi section, India. Since these fractures are not bound by sets of other brittle planes, the former are *not* brittle shear related

References

- Grasemann B, Stüwe K, Vannay J-C (2003) Sense and non-sense of shear in flanking structures. *J Struct Geol* 25:19–34
- Handy MR, Hirth G, Bürgmann R (2007) Continental fault structure and rheology from the frictional-to-viscous transition downward. In: Handy MR, Hirth G, Hovius N (eds) Chapter 6: Tectonic faults: agents of change on a dynamic earth. The MIT Press, Cambridge, pp 139–181
- Hippertt JFM (1993) ‘V’ pull-apart microstructures: a new shear sense indicator. *J Struct Geol* 15:1394–1403
- Mukherjee S (2010) Macroscopic V-pull apart structure in garnet. *J Struct Geol* 32:605
- Mukherjee S (2013) Higher Himalaya in the Bhagirathi section (NW Himalaya, India): its structures, backthrusts and extrusion mechanism by both channel flow and critical taper mechanisms. *Int J Earth Sci* 102:1851–1870
- Mukherjee S, Koyi HA (2010) Higher Himalayan Shear Zone, Sutlej section: structural geology and extrusion mechanism by various combinations of simple shear, pure shear and channel flow in shifting modes. *Int J Earth Sci* 99:1267–1303
- Passchier CW, Trouw RAJ (2005) *Microtectonics*, 2nd edn. Springer, Berlin
- Roy P, Jain AK, Singh S (2010) Microstructures of mylonites along the Karakoram Shear Zone, Tangste Valley, Pangong Mountains, Karakoram. *J Geol Soc Ind* 75:679–694
- Singh K (1996) Pull apart microstructures in feldspar from Chail thrust zone, Dhauladhar range, Western Himachal Pradesh. In: Jain AK, Manickavasagam RM (eds) *Geodynamics of the NW Himalaya*. *Gond Res Gp Mem* 6:117–23
- Tchalenko JS (1970) Similarities between shear Zones of different magnitudes. *Geol Soc Am Bull* 81:1625–1640